How pulse disturbances shape size-abundance pyramids

Claire Jacquet, Isabelle Gounand, Florian Altermatt

How pulse disturbances shape size-abundance pyramids

Claire Jacquet[1,2*], Isabelle Gounand[1,2,3], Florian Altermatt[1,2]

[1] Department of Aquatic Ecology, Swiss Federal Institute of Aquatic Science and Technology, Eawag, Dübendorf, Switzerland

[2] Department of Evolutionary Biology and Environmental Studies, University of Zurich, Zürich, Switzerland

[3] Sorbonne Université, CNRS, UPEC, CNRS, IRD, INRA, Institut d'écologie et des sciences de l'environnement, IEES,, Paris, France

* corresponding author: phone: +41 58 765 6726, fax: +41 58 765 5802

Authors' e-mail addresses: claire.jacquet@eawag.ch, isabelle.gounand@eawag.ch, florian.altermatt@eawag.ch

Statement of authorship: CJ and FA designed research, CJ conducted the experimental research, CJ and IG designed the theoretical research and IG did the mathematics and simulations to produce the theoretical figures. CJ wrote the first draft of the manuscript and all authors critically contributed to the edition of the paper.

1

Keywords: perturbations, extreme events, metabolic theory, body-size, community size-structure, size spectrum, protist communities, disturbance frequency, disturbance intensity.

Running title: How pulse disturbances shape size-abundance pyramids.

Type of article: Letter.

Abstract: 144 words.

Main text: 4750 words.

References: 67.

The manuscript contains 6 Figures and Supporting Information.

2

Abstract

Ecological pyramids represent the distribution of abundance and biomass of living organisms across body-sizes. Our understanding of their expected shape relies on the assumption of invariant steady-state conditions. However, most of the world's ecosystems experience disturbances that keep them far from such a steady state. Here, using the allometric scaling between population growth rate and body-size, we predict the response of size-abundance pyramids within a trophic guild to any combination of disturbance frequency and intensity affecting all species in a similar way. We show that disturbances narrow the base of size-abundance pyramids, lower their height and decrease total community biomass in a nonlinear way. An experimental test using microbial communities demonstrates that the model captures well the effect of disturbances on empirical pyramids. Overall, we demonstrate both theoretically and experimentally how disturbances that are not size-selective can nonetheless have disproportionate impacts on large species.

INTRODUCTION

Ecological pyramids, which represent the distribution of abundance and biomass of organisms across body-sizes or trophic levels, reveal one of the most striking regularities among communities (Elton 1927; Lindeman 1942; Trebilco *et al.* 2013). Several types of pyramids have been reported in ecological research, as well as distinct underlying mechanisms to explain their shape. For example, trophic pyramids describe the distribution of abundance or biomass along discrete trophic levels (Fig. 1a). The inefficiency in energy transfer from resources to consumers as well as strong self-regulation within trophic levels provide the main explanation for their shape (Lindeman 1942; Barbier & Loreau 2019). Alternatively, size-abundance pyramids (Fig. 1b,c), also known as the pyramid of numbers (Elton 1927), the Damuth law (Damuth 1981), or the abundance size spectrum (Sprules & Barth 2016), describe the distribution of abundance across body-sizes and can be studied both within and across trophic guilds (Elton 1927; Trebilco *et al.* 2013). The energetic equivalence rule, along with the metabolic theory of ecology, provide theoretical expectations regarding the shape of such size-abundance pyramids: in a community where all individuals feed on a common resource (i.e. within a trophic group), population abundance should be proportional to $M^{-0.75}$, where M is body-size, and biomass should be proportional to $M^{0.25}$ (Damuth 1981; Brown *et al.* 2004; White *et al.* 2007).

As with most concepts in ecology, these relationships correspond to theoretical baselines that are predicted under steady-state conditions, which are rarely met in nature (DeAngelis & Waterhouse 1987; Hastings 2004, 2010). Most natural ecosystems and communities are exposed to a wide range of environmental fluctuations and disturbances, ranging from harvesting to extreme weather events. Furthermore, many of these disturbances are expected to increase in frequency and intensity in the context of global change, as illustrated by recent large scale wildfires, floods or

hurricanes (Coumou & Rahmstorf 2012; Hughes *et al.* 2017; Harris *et al.* 2018). Such disturbances increase population mortality and could trigger even faster changes in community structure and dynamics than gradual changes in average conditions (Jentsch *et al.* 2009; Wernberg *et al.* 2013; Woodward *et al.* 2016).

Despite the extensive literature on disturbance ecology (Sousa 1984; Yodzis 1988; Petraitis *et al.* 1989; Fox 2013; Dantas *et al.* 2016; Thom & Seidl 2016), the effects of disturbances on community structure and biomass distribution remain poorly understood (Donohue *et al.* 2016). On the one hand, ecologists have often focused on the consequences of environmental disturbances on species richness (Huston 1979; Haddad *et al.* 2008; Bongers *et al.* 2009) and the coexistence of competing species (Violle *et al.* 2010; Miller *et al.* 2011; Fox 2013), rather than on body-size and biomass distribution (but see Woodward *et al.* (2016)). As such, the specific identity of species resistant (or not) to disturbances has received ample attention, with various definitions of disturbance-resistant species groups (Sousa 1980, 1984; Lavorel *et al.* 1997). These studies have pointed out key demographic traits, notably population growth rate and carrying capacity, that determine species' capacities to persist in a disturbed environment (McGill *et al.* 2006; Haddad *et al.* 2008; Enquist *et al.* 2015; Woodward *et al.* 2016). On the other hand, the metabolic theory of ecology uses the scaling of metabolic rate with body-size to predict a set of structural and functional characteristics across biological scales (Brown *et al.* 2004). At the community level, it demonstrates how size-abundance pyramids emerge from the scaling of population growth rate and abundance with body-size (Trebilco *et al.* 2013). Surprisingly, a formal integration of the theory on disturbances with the metabolic theory of ecology is still lacking, but would allow ecologists to generalize and predict the effect of environmental disturbances on the shape of size-abundance pyramids.

Here, we integrate these two disconnected fields by developing a size-based model for population persistence, assuming that the scaling of population growth rate with body-size is the leading mechanism determining the response of size-abundance pyramids to disturbances. We predict the shape of size-abundance pyramids within a trophic guild in response to repeated pulse disturbances of varying frequency and intensity affecting all species in a similar way, regardless of their size. Such disturbances represent a wide range of environmental pressures that increase species mortality, such as floods, wildfires, or hurricanes. They differ from the disturbance studies developed in fishery sciences, that specifically addressed the effect of a press, size-selective disturbance (i.e. fishing) on the abundance size spectrum (Jennings *et al.* 2002; Shin *et al.* 2005; Petchey & Belgrano 2010; Sprules & Barth 2016). We then experimentally test the predicted responses of size-abundance pyramids and standing biomass to disturbances, using microbial communities composed of aquatic species with body-sizes and populations densities varying over several orders of magnitudes. We finally discuss the general implications of our findings for the structure and functioning of communities exposed to environmental disturbances.

MATERIALS AND METHODS

A model for size-abundance pyramids exposed to disturbances

We build a mechanistic model to predict how disturbance frequency and intensity modulate the shape of size-abundance pyramids and community total biomass. We describe the dynamics of population abundance N with a logistic model:

$$\frac{dN}{dt} = rN\left(1 - \frac{N}{K}\right) \quad (1)$$

where r is population growth rate and K is population carrying capacity. We model a disturbance regime, corresponding to a recurrent abundance reduction, of intensity I (fraction of abundance)

and frequency f or period $T=1/f$ (time between two disturbances, Fig. 2a). We can demonstrate that a population persists in a disturbed environment only if its growth rate balances the long-term effect of the disturbance regime (adapted from Harvey *et al.* 2016), that is:

$$r > -\frac{\ln(1-I)}{T} \quad (2)$$

From equation (2), we can predict the set of disturbance regimes a population can sustain according to its growth rate (Fig. 2b), as well as the minimum generation time ($1/r$) needed to maintain a viable population (Fig. S1). We then use the allometric relationship between population growth rate r and average body-size M, that is $r = c \times M^a$ with $a = -¼$ (Brown *et al.* 2004; Savage *et al.* 2004) and c a positive constant, to derive the following size-specific criterion for population persistence under a disturbance regime:

$$M \leq \left(\frac{\ln(1-I)}{T \times c}\right)^{-4} \quad (3)$$

Equation (3) indicates that a species can persist in a disturbed environment only if its average body-size is below a certain value. Note that this analytical criterion is applicable to any biological and temporal scale. Indeed, the disturbance frequency and population growth rate are expressed with the same time unit and can range from hours (e.g. fast-growing microbial organisms) to years (e.g. slow-growing organisms such as large mammals). To investigate the effect of disturbances on the shape of size-abundance pyramids, we derive the mean abundance at dynamical equilibrium $\bar{N}$ of a population under a given disturbance regime (i.e. averaged over a time period, see Appendix 1 for detailed steps), that is:

$$\bar{N} = K\left(\frac{ln(1-I)}{T \times r} + 1\right) \quad (4)$$

where K corresponds to the carrying capacity of the population, which also scales with body-size on a logarithmic scale (Brown & Gillooly 2003; Brown *et al.* 2004): $ln(K) = a_K \ln(M) + b_K$,

where a_K and b_K are normalizing constants. We use this allometric relationship to express mean abundance as a function of mean population body-size and finally obtain:

$$ln(\bar{N}) = a_K \ln(M) + b_K + ln\left(\frac{ln(1-I)}{Te^{a_r \ln(M) + b_r}} + 1\right) \quad (5)$$

The formula is valid when the expression in parentheses in the right-hand term is positive, which corresponds to the persistence criteria given in equations (2) and (3). We express population biomass, *B,* as the product of mean abundance at dynamical equilibrium, $\bar{N}$, and the average individual body-size in the population, M, that is $B = \bar{N}M$.

We extend this approach to multispecies assemblages composed of potentially hundreds of co-occurring species with different body-sizes (see detailed method in Appendix 2 and Table S1 for parameter values). We assume that all species' populations follow a logistic growth and are constrained by intraspecific competition only (an assumption relaxed in Appendix 3). From equation (3) and (5), we expect that disturbances will decrease the maximum size observed in the community as well as total biomass. We use this analytical approach to explore how community size-structure, a more tractable representation of abundance distribution across size-classes compared to pyramids (Fig. 1b), and total community biomass will respond to a whole landscape of disturbance frequencies and intensities (Fig. 3).

Disturbance experiment on microbial communities

We conducted an experiment in aquatic microcosms inoculated with 13 protist species and a set of common freshwater bacteria as a food resource. The protist species cover a wide range of body-sizes (from 10–10^3 µm) and densities (10–10^5 individuals/ml, Giometto *et al.* 2013). General lab procedures follow the protocols described in Altermatt *et al.* (2015), and build upon previous work on pulse disturbance effects on diversity (Altermatt *et al.* 2011; Harvey *et al.* 2016) and

131 invasion dynamics (Mächler & Altermatt 2012). Detailed microcosm description and set-up are
132 presented in Appendix 4. In short, we performed a factorial experiment in which we varied
133 disturbance frequency and intensity, resulting in a total of twenty different disturbance regimes.
134 Disturbance was achieved by boiling a subsampled fraction of the well-mixed community in a
135 microwave so that all species experience the same level of density reduction. All protists were
136 killed by the microwaving process. We let the medium cool down before putting it back into the
137 microcosm. We disturbed microcosms at five intensities: 10, 30, 50, 70 and 90 % and at four
138 frequencies: f = 0.08, 0.11, 0.16 and 0.33, corresponding to a disturbance every 12, 9, 6 and 3 days,
139 respectively. The experiment lasted for 21 days, or about 10–50 generations depending on species.
140 Each disturbance regime was replicated six times. To control for the intrinsic variability of
141 community size-structure, we cultured eight undisturbed microcosms under the same conditions.
142 We sampled 0.2 ml of each microcosm daily to quantify individual body-sizes (i.e. cell area in
143 μm^2), protist abundances (individuals/µl) and total community biomass (i.e. total bioarea in
144 $\mu m^2/\mu l$) using a standardized video procedure (Altermatt *et al.* 2015; Pennekamp *et al.* 2017). We
145 binned the observed individuals into twelve size-classes ranging from 0 to 1.6×10^5 μm^2 in order to
146 get statistically comparable community size-structures. Mean protist abundance and its standard
147 deviation in each size-class were calculated over 21 time points and 6 replicates (total of 126
148 observations) for each treatment and over 21 time points and 8 replicates (total of 168 observations)
149 for the control communities. We performed Welch two sample t-tests of mean comparison
150 (treatment versus control) to determine which disturbance regime had a significant effect on
151 community size-structure and total community biomass (Table S2).
152
153 **Model parameterization**

We parameterized the model using the experimental data in order to test the capacity of the model to predict the effect of a given disturbance regime on the size-structure of real communities. The model required the following input parameters: the carrying capacities of each size-class as well as the slope and the intercept of the allometric relationship between growth rate and body-size. We took the average abundances of the undisturbed communities (8 controls) to the estimate carrying capacities in each size-class. We fitted a logistic growth model to the recovery dynamics of each size-class after one disturbance (I = 90%) to obtain growth rate estimations. Specifically, we used the data from the treatment $\{I$=90%, f =0.08$\}$ (i.e. highest intensity, lowest frequency) to estimate the parameters of a logistic growth model over 12 time points using the function *nls*() of the *stats* package in R (R Core Team 2019). We determined the relationship between growth rate and body-size in our experimental communities using the 13 time-series (covering 6 size-classes) that displayed a logistic growth. We obtained the following allometric relationship: $ln(r) = -0.37 \times \ln(M) + 3.75$ (p-value = 0.005, R^2 = 0.47). Using this parameterization, we produced theoretical predictions on the size-abundance pyramids expected in the experimental disturbance regimes. We then quantitively compared these predictions with the size-abundance pyramids observed in the experimental communities. We performed ordinary least-squares regressions to characterize the relationship between observed and predicted log-transformed mean abundances among size-classes for all the disturbance regimes.

RESULTS

Model predictions

We first explore the effects of increasing disturbance frequency (Fig. 3a, c). Infrequent disturbances do not strongly affect community size-structure and only decrease the mean abundance of the largest size-classes (Fig. 3a, f = 0.1 in dark blue). Maximum body-size gradually

178 decreases as disturbance frequency increases, corresponding to the extinction of large, slow-
179 growing species (Fig. 3a, $f = 0.25$ in light blue). Disturbance frequency also affects the community
180 size-structure through its effect on mean abundance. For frequent disturbance events, the mean
181 abundance of all size-class decreases (Fig. 3a, $f = 0.5$ and 1 in orange and red respectively). The
182 effect of disturbance frequency on community-size structure have direct consequences for
183 community-level properties: we indeed observe an approximately linear decrease in total
184 community biomass (log) along a gradient of disturbance frequency, followed by an abrupt collapse
185 of the community for extreme disturbance regimes (Fig. 3c).

186 We then investigate the effect of increasing disturbance intensity (Fig. 3b, d). Similarly,
187 low intensity disturbances marginally affect community size-structure (Fig. 3c, $I = 30\%$ in blue)
188 and increasing disturbance intensity decreases maximum body-size and population mean
189 abundance. (Fig. 3b). Interestingly, the effect of disturbance intensity on community total biomass
190 is clearly nonlinear (Fig. 3d). Low to intermediate disturbance intensities do not affect total biomass
191 when disturbance frequency is low (e.g. $f = 0.1$ or 0.25 in Fig. 3d). However, strong intensities
192 affect all population abundances and trigger a sharp decrease in total biomass, culminating in a
193 crash of the system (e.g. $\{I > 90\%, f = 0.25\}$ in Fig 3d).

194

195 **Experimental results**

196 We experimentally investigated the effect of disturbance frequency and intensity on the
197 size-structure of microbial communities. For a fixed intensity (set to $I = 90\%$ in Fig. 4a, see Fig.
198 S2 for other intensities), infrequent disturbances (i.e. $f = 0.08$ and $f = 0.11$) had a significant
199 negative impact only on the mean abundance of intermediate size-classes (between exp(9.6) and
200 exp(10.5) μm^2, Welch two sample t-tests: $t \geq 2.6$, p-values ≤ 0.02, Table S2). When disturbance

frequency increased to $f = 0.16$, the mean abundance of the smallest size-class also decreased ($t = 3.6$, p-value = 0.01, Table S2). Finally, at even more frequent disturbances ($f = 0.33$), all size-classes were negatively impacted, except the smallest one (Fig 5a and Table S3). Overall, increasing disturbance frequency led to an abundance depletion at intermediate sizes compared to undisturbed control communities.

Similarly, for a fixed frequency (set to $f = 0.33$ in Fig. 4b, see Fig. S3 for other frequencies), a low disturbance intensity $I = 10$ % (Fig. 4b) only affected intermediate size-classes (between exp(10) and exp(10.5) μm^2, $t \geq 4.5$, p-values ≤ 0.001, Table S2). Disturbance intensities $I = 30\%$ and 50% had a negative effect on the mean abundance of larger size-classes (between exp(10) and exp(11) μm^2, $t \geq 2.8$, p-values ≤ 0.03, Table S2). Finally, intensities $I = 70\%$ and $I = 90\%$ had an impact on all size-classes, except the smallest size-class that were not negatively impacted by change in disturbance intensity (Fig. 4b, Table S2). Interestingly, the following disturbance regimes had a positive effect of on the mean abundance of the smallest size-class: $\{I = 30\%, f = 0.33\}$, $t = -6.1$, p-value < 0.001, (Fig. 4b), as well as $\{I = 50\%, f = 0.16\}$ and $\{I = 70\%, f = 0.11\}$ (Table S2, Fig. S2 and S3).

At the community-level, total biomass gradually decreased with disturbance frequency as expected by theory (Fig. 4c). All frequencies had a significant negative effect on total biomass compared to controls ($t \geq 8$, p-value < 0.001, Fig 4c). Disturbance intensities $I = 10\%$ and 30% had no significant effects on total community biomass ($I_{10\%}$: $t = 0.75$, p-value = 0.48, $I_{30\%}$: $t = 0.5$, p-value = 0.63), while total biomass strongly decreased for intensities above $I = 50\%$ ($I_{50\%}$: $t = 6.1$, p-value < 0.001, $I_{70\%}$: $t = 12.7$, p-value < 0.001, $I_{90\%}$: $t = 14.2$, p-value < 0.001, Fig. 4d).

Observed versus predicted effect of disturbances on size-abundance pyramids

We then compared our experimental results with the predictions of the model parameterized for our freshwater microbial communities (Figure 5). The model predicted well the observed mean abundances relative to carrying capacity for all the disturbance regimes in most of the size-classes. The slope of the linear regression between observed and predicted log mean abundances, including all size-classes in all disturbance regimes (240 points), was very close to the 1:1 line, which indicates a very good fit (Figure 5a, linear regression: $y = -0.012 + 1.01x$, $R^2 = 0.96$, p-value < 0.001). Additionally, the intercept of the linear regression was not significantly different from zero ($t = 0.95$, p-value = 0.34). We illustrate in Figure 5b-d the similarities as well as the differences between the predicted and observed community size-structures for varying disturbance frequencies with a disturbance intensity fixed to $I = 90\%$ (other disturbance regimes are shown in Figs. S4-S5). Overall, the predicted community structures were very similar to the observed ones. The model, however, often underestimated the mean abundance in the smallest size-class (Figure 5d). Furthermore, as mentioned in the previous section, some disturbance regimes had a positive effect of on the mean abundance of the smallest size-class, which cannot, by construction, be predicted by our model. We discuss below how this pattern can be explained by a disruption of biotic interactions following a disturbance and present further analyses using a predator-prey model to support this possible explanation (Fig. 6c, Appendix 3).

DISCUSSION

Most theories in community ecology have been developed under the assumption of steady-state conditions (Hastings 2010). Yet, most of the world's ecosystems – specifically ≥75% of land/freshwater and 50% of marine systems – have been altered by human activities and are facing disturbances that put them clearly outside of such a steady state (IPBES 2018). Thus, to meet the societal demand for an ecological science able to predict how ecosystems will respond to global

248 change (Petchey *et al.* 2015; Urban *et al.* 2016), this assumption needs to be relaxed. The challenge
249 is to develop models that make quantitative predictions regarding the impact of fluctuating
250 environmental conditions on the structural and functional characteristics of biological systems.
251
252 **Consequences of the growth-size relationship for communities exposed to disturbances**
253 Here, we provide a robust and simple approach for predicting the size-structure of
254 communities exposed to any combination of disturbance frequency and intensity affecting all
255 species in a similar way, regardless of their body-size. We combine theory on disturbances with
256 the metabolic theory of ecology and assume that the scaling of population growth rate with body-
257 size is the leading mechanism determining the response of size-abundance pyramids to
258 disturbances. The model makes an important advance over the steady-state predictions of the
259 metabolic theory of ecology as it links quantitatively the shape of a size-abundance pyramid to the
260 disturbance regime experienced by the community (Fig. 6a–b). Overall, increasing disturbance
261 frequency or intensity narrows the bases of size-abundance pyramids and lowers their height. This
262 corresponds to the extinction of the largest species and a general reduction of population mean
263 abundances in all size-classes. Hence, we demonstrate that disturbances that are not size-selective
264 and do not target large species have nonetheless a higher impact on large species than on smaller
265 ones.
266 The model is applicable across all biological and temporal scales as population growth rate
267 and disturbance frequency are expressed with the same time units. Equation (2) can also apply to
268 populations that do not show a scaling relationship between growth rate and body-size and predicts
269 which disturbance regimes a species can sustain, or not, based on its generation time (Figs. 2 and
270 S1). Importantly, our results are not specific to repeated pulse disturbances but also hold for press

disturbances, which will affect the shape of size-abundance pyramids in an equivalent way (see Appendix 1 for a mathematical demonstration).

Our model offers a new perspective on community responses to disturbances by exploring the effect of repeated pulse disturbances of varying frequency and intensity on community size structure. The majority of theoretical studies on community stability have focused on local stability, which examine community's response to small pulse disturbances around one single equilibrium (Donohue *et al.* 2016), reflecting the great interest for the so-called diversity-stability debate (May 1972; McCann 2000; Allesina & Tang 2012; Jacquet *et al.* 2016). Our approach goes beyond local stability measures at the vicinity of one single attractor and is applicable to any combination of disturbance frequency or intensity. It predicts which species, based on its growth rate, can persist or not and how the abundances of the remaining species will be affected by a whole gradient of disturbances.

Note that the model depends on a number of technical assumptions. First, we restricted our theoretical approach to disturbance regimes where pulse disturbances are applied at fixed intervals with a fixed intensity. This choice, though relatively simplistic, allowed us to mirror the disturbance regimes applied to the experimental communities. To generalize, we also performed simulations where we added stochasticity in the frequency and intensity of the disturbance regime to test the sensitivity of the theoretical results to variability in the periodicity and intensity of disturbances (Appendix 2). Our results were qualitatively robust to the addition of noise around average values of disturbance frequency and intensity, which simply increased the negative effect of one given disturbance regime on the largest size-classes (Fig. S6). Second, we consider that the allometric parameters of the relationships between population growth rate, carrying capacity and body-size are the same for all species (i.e. same slopes and intercepts). We therefore performed sensitivity

294 analyses of Equation (5) and demonstrate that our results are robust to variation in these allometric
295 parameters (Appendix 2, Fig. S7-8).
296
297 **Experimental test of the theory**
298 The disturbance experiment on microbial communities showed some similarities but also
299 some departures from the theoretical predictions (Figure 5b-d). As expected from the analytical
300 model, total community biomass gradually decreased with disturbance frequency and in a more
301 nonlinear way with disturbance intensity (Fig. 4c–d, and Fig. 3c–d for the theoretical predictions).
302 Interestingly, it was the intermediate and not the largest size-classes that were the most sensitive
303 to disturbances in the microbial community. We provide below two possible explanations for this
304 observation. Most likely, the abundances of the largest size-class might be already too low, and
305 therefore too close to the methodologically-defined detection threshold, in the control communities
306 to observe a significant effect of the disturbances of these size-classes. Second, this might be
307 explained by the duration of the experiment (21 days), which was not long enough to capture the
308 extinction of the largest species. We estimated the time to reach the dynamical equilibrium in the
309 experiment with the model parameterized with experimental data (see Table S3). The model
310 predicted that equilibrium is reached by the end of the experiment (21 days) for the size-classes
311 considered in all disturbance regimes but the strongest. With the highest frequency and intensity
312 $\{I=90\%; f=0.33\}$ the equilibrium is reached by the three smallest size-classes (in 12, 18, and 21
313 days respectively).
314 Additionally, some combinations of disturbance frequency and intensity had a positive
315 effect on the smallest size-class of microbes compared to controls, which corresponded to the main
316 departure from the theoretical predictions (Figure 4a-b and Figure 5d). This could be explained by
317 a disruption of biotic interactions (predation or competition) following a disturbance, allowing the

318 remaining small species to grow in higher densities in the absence of other species (Cox & Ricklefs
319 1977; Ritchie & Johnson 2009; Bolnick *et al.* 2010). Such "interaction-release" mechanism could
320 not be captured by our model of co-occurring species. We discuss below how interspecific
321 interactions, such as competition, predation or parasitism, could modulate the shape of size-
322 abundance pyramids exposed to disturbances.
323
324 **Extending the model to communities of interacting species**
325 To observe an "interaction-release" effect that will widen the pyramid's base, two
326 conditions are required (but not sufficient): (i) the existence of a significant mismatch between the
327 growth rates of the two interacting species, leading to differential response to disturbances, and (ii)
328 the species with the slowest growth rate has a negative effect on the other species (i.e. predator,
329 competitor or parasite). The latter condition seems unlikely for parasitism. For competitive
330 interactions, a "competition-release" effect can potentially increase the abundance of small, fast-
331 growing species that will recover faster from a disturbance event compared to larger competitors
332 (e.g. Xi *et al.* (2019)). Finally, the existence of a "predation-release" effect is very likely as
333 predators are generally larger than their prey and have slower growth rates (Brose *et al.* 2006, 2016;
334 Barnes *et al.* 2010). In an additional analysis, we performed simulations using a predator-prey
335 model to explore in which conditions a "predation-release" effect could increase the abundance of
336 small prey species (see Appendix 3 for detailed methods). We found that small to intermediate
337 disturbance regimes can increase average prey abundance through a "predation-release" effect,
338 which should generate size-abundance pyramids with a wider base (Fig. 6c). This effect vanishes
339 above some disturbance thresholds, where prey species are also negatively impacted by
340 disturbances (Fig. 6c and Figs. S9-S11).

Our model cannot capture cascading effects triggered by complex interactions networks in its current form. A promising future direction is the extension of the model to multitrophic communities, which will allow further explorations of the potential of interspecific interactions to modulate the impact of disturbances on size-abundance pyramids and community biomass. Indeed, it is likely that predator species will also be impacted indirectly through a bottom-up transmission of the disturbances (i.e. decrease in prey availability).

Additional mechanisms shaping size-abundance pyramids exposed to disturbances

Here, we propose a systematic approach, based on the metabolic theory of ecology, to predict the response of size-abundance pyramids to persistent disturbances. Our results are specific to a class of persistent disturbances (i.e. pulse or press) that affect the abundance of all species in a similar way, regardless of their specific body-size or growth rate. We also assume that the leading mechanism that determines the response of size-abundance pyramids to this type of disturbances is the allometric relationship between species growth rate and body-size. However, additional mechanisms can generate size-dependent abundances or size-dependent responses to disturbances in real world ecosystems. First, species sensitivity to disturbances that are not size-selective can be nonetheless unequal among size classes, with particular size-classes being more resistant to a given disturbance intensity. For example, strong windstorms or droughts generally cause greater mortality among larger or taller trees (Woods 2004; Hurst *et al.* 2011; Bennett *et al.* 2015). Second, from a spatial perspective, size-specific mobility and immigration-extinction dynamics could largely affect the relationship between species recovery dynamics and their size (McCann *et al.* 2005; Jacquet *et al.* 2017). It would be interesting to extend our approach to metacommunities, where the depletion of large species in a disturbed habitat patch could be balanced by immigration from undisturbed neighboring patches (Pawar 2015).

365 Finally, some disturbances can be size-selective, as illustrated by studies on abundance size
366 spectra that specifically addressed the effect of a press, size-selective disturbance, often reflecting
367 disturbances expected under commercial fishing (Shin *et al.* 2005; Sprules & Barth 2016). Our
368 model can easily be refined to more specific cases, in which disturbances have unequal effects on
369 species, by adding size-specific disturbance intensities to the model. The abundance size spectra
370 of harvested fish communities are generally characterized by steeper slopes than unfished
371 communities, and are used as a size-based indicator of fisheries exploitation (Shin *et al.* 2005;
372 Petchey & Belgrano 2010; Sprules & Barth 2016). We demonstrate that size-abundance pyramids
373 are also predictably affected by more general pulse disturbances that are not size-selective such as
374 floods or wildfires. Hence, when compared to a reference state, size-abundance pyramids provide
375 information on the level of disturbances an ecosystem is facing and could be used as "universal
376 indicators of ecological status", as advocated in Petchey & Belgrano (2010).
377
378 **Conclusion**
379 Our findings have direct implications regarding the effects of disturbances on ecosystem
380 functioning. Indeed, the model makes predictions on total biomass and demographic traits
381 correlated to productivity rate and energy flows, which are among the most relevant metrics to
382 quantify ecosystem functioning (Oliver *et al.* 2015; Schramski *et al.* 2015; Brose *et al.* 2016;
383 Barnes *et al.* 2018). In the current context of global change, we demonstrate that the expected
384 increase in disturbance frequency and intensity should accelerate the extinction of the largest
385 species, leading to an increasing proportion of communities dominated by small, fast-growing
386 species and lower levels of standing biomass. Importantly, the effect of increasing disturbance
387 regimes will be nonlinear and abrupt changes in community structure and functioning are expected
388 once a disturbance threshold affecting the equilibrium abundances of smaller species is reached.

DATA AVAILABILITY STATEMENT

The data supporting the experimental results as well as a Rmarkdown document, which explains in detail the theoretical approach and produces the figures, are archived in the Dryad Digital Repository: https://doi.org/10.5061/dryad.95x69p8g7.

ACKNOWLEDGEMENT

We thank Sereina Gut, Samuel Hürlemann and Silvana Käser for help during the laboratory work and Chelsea J. Little for comments on the manuscript. We also thank Jean François Arnoldi, Samraat Pawar and two anonymous reviewers for their helpful comments on previous versions of the manuscript. Funding is from the Swiss National Science Foundation Grants No PP00P3_179089, the University of Zurich Research Priority Program "URPP Global Change and Biodiversity" (both to F.A.) and the University of Zurich Forschungskredit (to C.J. and I.G.).

REFERENCES

Allesina, S. & Tang, S. (2012). Stability criteria for complex ecosystems. *Nature*, 483, 205–208.

Altermatt, F., Fronhofer, E.A., Garnier, A., Giometto, A., Hammes, F., Klecka, J., *et al.* (2015). Big answers from small worlds: a user's guide for protist microcosms as a model system in ecology and evolution. *Methods Ecol. Evol.*, 6, 218–231.

Altermatt, F., Schreiber, S. & Holyoak, M. (2011). Interactive effects of disturbance and dispersal directionality on species richness and composition in metacommunities. *Ecology*, 92, 859–870.

Barbier, M. & Loreau, M. (2019). Pyramids and cascades: a synthesis of food chain functioning and stability. *Ecol. Lett.*, 22, 405–419.

413 Barnes, A.D., Jochum, M., Lefcheck, J.S., Eisenhauer, N., Scherber, C., O'Connor, M.I., *et al.*
414 (2018). Energy Flux: The Link between Multitrophic Biodiversity and Ecosystem
415 Functioning. *Trends Ecol. Evol.*, 33, 186–197.
416 Barnes, C., Maxwell, D., Reuman, D.C. & Jennings, S. (2010). Global patterns in predator —
417 prey size relationships reveal size dependency of trophic transfer efficiency. *Ecology*, 91,
418 222–232.
419 Bennett, A.C., McDowell, N.G., Allen, C.D. & Anderson-Teixeira, K.J. (2015). Larger trees
420 suffer most during drought in forests worldwide. *Nat. Plants*, 1, 15139.
421 Bolnick, D.I., Ingram, T., Stutz, W.E., Snowberg, L.K., Lau, O.L. & Paull, J.S. (2010).
422 Ecological release from interspecific competition leads to decoupled changes in population
423 and individual niche width. *Proc. R. Soc. B*, 277, 1789–1797.
424 Bongers, F., Poorter, L., Hawthorne, W.D. & Sheil, D. (2009). The intermediate disturbance
425 hypothesis applies to tropical forests, but disturbance contributes little to tree diversity. *Ecol.*
426 *Lett.*, 12, 798–805.
427 Brose, U., Blanchard, J.L., Eklöf, A., Galiana, N., Hartvig, M., R. Hirt, M., *et al.* (2016).
428 Predicting the consequences of species loss using size-structured biodiversity approaches.
429 *Biol. Rev.*, 49, n/a-n/a.
430 Brose, U., Jonsson, T. & Berlow, E.L. (2006). Consumer-resource body size relationships in
431 natural food webs. *Ecology*, 87, 2411–2417.
432 Brown, J.H. & Gillooly, J.F. (2003). Ecological food webs : High-quality data facilitate
433 theoretical unification. *Proc. Natl. Acad. Sci.*, 100, 1467–1468.
434 Brown, J.H., Gillooly, J.F., Allen, A.P. & Savage, V.M. (2004). Toward a metabolic theory of
435 ecology. *Ecology*, 85, 1771–1789.
436 Coumou, D. & Rahmstorf, S. (2012). A decade of weather extremes. *Nat. Clim. Chang.*, 2, 491–

496.

Cox, G.W. & Ricklefs, R.E. (1977). Species Diversity and Ecological Release in Caribbean Land Bird Faunas. *Oikos*, 28, 113.

Damuth, J. (1981). Population density and body size in mammals. *Nature*, 290, 699–700.

Dantas, V. de L., Hirota, M., Oliveira, R.S. & Pausas, J.G. (2016). Disturbance maintains alternative biome states. *Ecol. Lett.*, 19, 12–19.

DeAngelis, D.L. & Waterhouse, J.C. (1987). Equilibrium and Nonequilibrium Concepts in Ecological Models. *Ecol. Monogr.*, 57, 1–21.

Donohue, I., Hillebrand, H., Montoya, J.M., Petchey, O.L., Pimm, S.L., Fowler, M.S., *et al.* (2016). Navigating the complexity of ecological stability. *Ecol. Lett.*, 19, 1172–1185.

Elton, C. (1927). *Animal Ecology*. Macmillan.

Enquist, B.J., Norberg, J., Bonser, S.P., Violle, C., Webb, C.T., Henderson, A., *et al.* (2015). Scaling from Traits to Ecosystems: Developing a General Trait Driver Theory via Integrating Trait-Based and Metabolic Scaling Theories. *Adv. Ecol. Res.*, 52, 249–318.

Fox, J.W. (2013). The intermediate disturbance hypothesis should be abandoned. *Trends Ecol. Evol.*, 28, 86–92.

Giometto, A., Altermatt, F., Carrara, F., Maritan, A. & Rinaldo, A. (2013). Scaling body size fluctuations. *Proc. Natl. Acad. Sci.*, 110, 4646–4650.

Haddad, N.M., Holyoak, M., Mata, T.M., Davies, K.F., Melbourne, B.A. & Preston, K. (2008). Species' traits predict the effects of disturbance and productivity on diversity. *Ecol. Lett.*, 11, 348–356.

Harris, R.M.B., Beaumont, L.J., Vance, T.R., Tozer, C.R., Remenyi, T.A., Perkins-Kirkpatrick, S.E., *et al.* (2018). Biological responses to the press and pulse of climate trends and extreme events. *Nat. Clim. Chang.*, 8, 579–587.

461 Harvey, E., Gounand, I., Ganesanandamoorthy, P. & Altermatt, F. (2016). Spatially cascading
462 effect of perturbations in experimental meta-ecosystems. *Proc. R. Soc. B*, 283, 20161496.
463 Hastings, A. (2004). Transients: the key to long-term ecological understanding? *Trends Ecol.*
464 *Evol.*, 19, 39–45.
465 Hastings, A. (2010). Timescales, dynamics, and ecological understanding. *Ecology*, 91, 3471–
466 3480.
467 Hughes, T.P., Kerry, J.T., Álvarez-Noriega, M., Álvarez-Romero, J.G., Anderson, K.D., Baird,
468 A.H., *et al.* (2017). Global warming and recurrent mass bleaching of corals. *Nature*, 543,
469 373–377.
470 Hurst, J.M., Allen, R.B., Coomes, D.A. & Duncan, R.P. (2011). Size-Specific Tree Mortality
471 Varies with Neighbourhood Crowding and Disturbance in a Montane Nothofagus Forest.
472 *PLoS One*, 6, e26670.
473 Huston, M. (1979). A General Hypothesis of Species Diversity. *Am. Nat.*, 113, 81–101.
474 IPBES. (2018). *Summary for policymakers of the global assessment report on biodiversity and*
475 *ecosystem services of the Intergovernmental Science-Policy Platform on Biodiversity and*
476 *Ecosystem Services*.
477 Jacquet, C., Moritz, C., Morissette, L., Legagneux, P., Massol, F., Archambault, P., *et al.* (2016).
478 No complexity–stability relationship in empirical ecosystems. *Nat. Commun.*, 7, 12573.
479 Jacquet, C., Mouillot, D., Kulbicki, M. & Gravel, D. (2017). Extensions of Island Biogeography
480 Theory predict the scaling of functional trait composition with habitat area and isolation.
481 *Ecol. Lett.*, 20, 135–146.
482 Jennings, S., Warr, K.J. & Mackinson, S. (2002). Use of size-based production and stable isotope
483 analyses to predict trophic transfer efficiencies and predator-prey body mass ratios in food
484 webs. *Mar. Ecol. Prog. Ser.*, 240, 11–20.

485 Jentsch, A., Kreyling, J., Boettcher-Treschkow, J. & Beierkuhnlein, C. (2009). Beyond gradual
486 warming: Extreme weather events alter flower phenology of European grassland and heath
487 species. *Glob. Chang. Biol.*, 15, 837–849.
488 Lavorel, S., McIntyre, S., Landsberg, J. & Forbes, T.D.A. (1997). Plant functional classifications:
489 from general groups to specific groups based on response to disturbance. *Trends Ecol. Evol.*,
490 12, 474–478.
491 Lindeman, R. (1942). The trophic-dynamic aspect of ecology. *Ecology*, 23, 399–417.
492 Mächler, E. & Altermatt, F. (2012). Interaction of Species Traits and Environmental Disturbance
493 Predicts Invasion Success of Aquatic Microorganisms. *PLoS One*, 7.
494 May, R.M. (1972). Will a large complex system be stable? *Nature*, 238, 413–4.
495 McCann, K.S. (2000). The diversity-stability debate. *Nature*, 405, 228–233.
496 McCann, K.S., Rasmussen, J.B. & Umbanhowar, J. (2005). The dynamics of spatially coupled
497 food webs. *Ecol. Lett.*, 8, 513–23.
498 McGill, B., Enquist, B.J., Weiher, E. & Westoby, M. (2006). Rebuilding community ecology
499 from functional traits. *Trends Ecol. Evol.*, 21, 178–85.
500 Miller, A.D., Roxburgh, S.H. & Shea, K. (2011). How frequency and intensity shape diversity-
501 disturbance relationships. *Proc. Natl. Acad. Sci.*, 108, 5643–5648.
502 Oliver, T.H., Heard, M.S., Isaac, N.J.B., Roy, D.B., Procter, D., Eigenbrod, F., *et al.* (2015).
503 Biodiversity and Resilience of Ecosystem Functions. *Trends Ecol. Evol.*, 30, 673–684.
504 Pawar, S. (2015). *The Role of Body Size Variation in Community Assembly*. *Trait. Ecol. - From*
505 *Struct. to Funct.* 1st edn. Elsevier Ltd.
506 Pennekamp, F., Griffiths, J.I., Fronhofer, E.A., Garnier, A., Seymour, M., Altermatt, F., *et al.*
507 (2017). Dynamic species classification of microorganisms across time, abiotic and biotic
508 environments—A sliding window approach. *PLoS One*, 12, e0176682.

509 Petchey, O.L. & Belgrano, A. (2010). Body-size distributions and size-spectra: universal
510 indicators of ecological status? *Biol. Lett.*, 6, 434–437.
511 Petchey, O.L., Pontarp, M., Massie, T.M., Kéfi, S., Ozgul, A., Weilenmann, M., *et al.* (2015).
512 The ecological forecast horizon, and examples of its uses and determinants. *Ecol. Lett.*, 18,
513 597–611.
514 Petraitis, P.S., Latham, R.E. & Niesenbaum, R.A. (1989). The Maintenance of Species Diversity
515 by Disturbance. *Q. Rev. Biol.*, 64, 393–418.
516 Ritchie, E.G. & Johnson, C.N. (2009). Predator interactions, mesopredator release and
517 biodiversity conservation. *Ecol. Lett.*, 12, 982–998.
518 Savage, V.M., Gillooly, J.F., Brown, J.H. & Charnov, E.L. (2004). Effects of body size and
519 temperature on population growth. *Am. Nat.*, 163, 429–41.
520 Schramski, J.R., Dell, A.I., Grady, J.M., Sibly, R.M. & Brown, J.H. (2015). Metabolic theory
521 predicts whole-ecosystem properties. *Proc. Natl. Acad. Sci.*, 112, 2617–2622.
522 Shin, Y.-J., Rochet, M.-J., Jennings, S., Field, J.G. & Gislason, H. (2005). Using size-based
523 indicators to evaluate the ecosystem effects of fishing. *ICES J. Mar. Sci.*, 62, 384–396.
524 Sousa, W.P. (1980). The responses of a community to disturbance: the importance of
525 successional age and species' life histories. *Oecologia*, 45, 72–81.
526 Sousa, W.P. (1984). The Role of Disturbance in Natural Communities. *Annu. Rev. Ecol. Syst.*, 15,
527 353–391.
528 Sprules, W.G. & Barth, L.E. (2016). Surfing the biomass size spectrum: Some remarks on
529 history, theory, and application. *Can. J. Fish. Aquat. Sci.*, 73, 477–495.
530 Thom, D. & Seidl, R. (2016). Natural disturbance impacts on ecosystem services and biodiversity
531 in temperate and boreal forests. *Biol. Rev. Camb. Philos. Soc.*, 91, 760–781.
532 Trebilco, R., Baum, J.K., Salomon, A.K. & Dulvy, N.K. (2013). Ecosystem ecology: size-based

533 constraints on the pyramids of life. *Trends Ecol. Evol.*, 28, 423–431.
534 Urban, M.C., Bocedi, G., Hendry, A.P., Mihoub, J.-B., Peer, G., Singer, A., *et al.* (2016).
535 Improving the forecast for biodiversity under climate change. *Science (80-.).*, 353,
536 aad8466–aad8466.
537 Violle, C., Pu, Z. & Jiang, L. (2010). Experimental demonstration of the importance of
538 competition under disturbance. *Proc. Natl. Acad. Sci.*, 107, 12925–12929.
539 Wernberg, T., Smale, D.A., Tuya, F., Thomsen, M.S., Langlois, T.J., De Bettignies, T., *et al.*
540 (2013). An extreme climatic event alters marine ecosystem structure in a global biodiversity
541 hotspot. *Nat. Clim. Chang.*, 3, 78–82.
542 White, E.P., Ernest, S.K.M., Kerkhoff, A.J. & Environnement, E.T. (2007). Relationships
543 between body size and abundance in ecology. *Trends Ecol. Evol.*, 22, 323–30.
544 Woods, K.D. (2004). Intermediate disturbance in a late-successional hemlock-northern hardwood
545 forest. *J. Ecol.*, 92, 464–476.
546 Woodward, G., Bonada, N., Brown, L.E., Death, R.G., Durance, I., Gray, C., *et al.* (2016). The
547 effects of climatic fluctuations and extreme events on running water ecosystems. *Philos.*
548 *Trans. R. Soc.*, 371, 20150274.
549 Xi, W., Peet, R.K., Lee, M.T. & Urban, D.L. (2019). Hurricane disturbances, tree diversity, and
550 succession in North Carolina Piedmont forests, USA. *J. For. Res.*, 30, 219–231.
551 Yodzis, P. (1988). The Indeterminacy of Ecological Interactions as Perceived Through
552 Perturbation Experiments. *Ecology*, 69, 508–515.
553

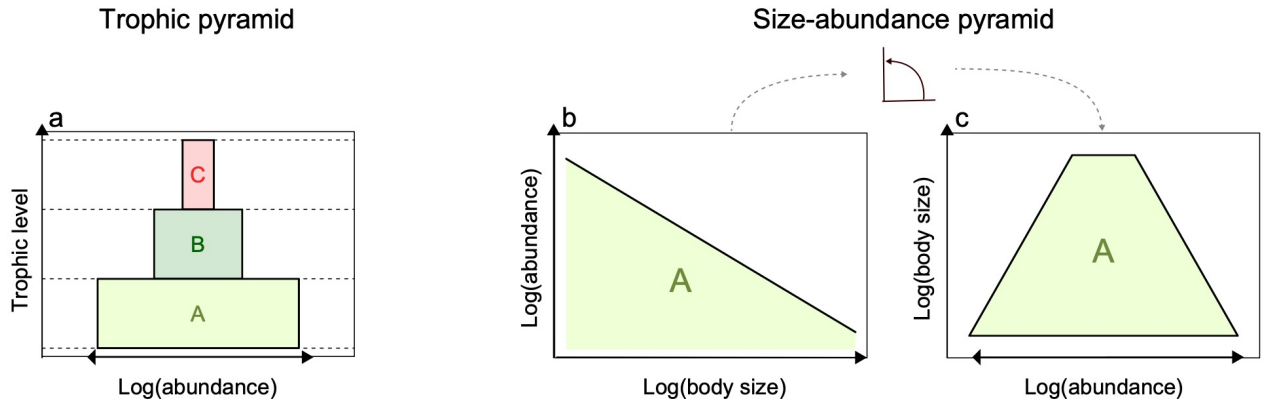

554

555

556 **Figure 1:** A trophic pyramid (a) describes the distribution of biomass along discrete trophic levels,
557 and assumes that all species within a trophic level have the same functional traits. The community
558 size-structure (b) and the size-abundance pyramid (c) are equivalent size-centric representations of
559 ecological communities and are the focus of this study. They describe the distribution of abundance
560 across body-sizes and can be studied both within and across trophic levels. b) the community size-
561 structure depicts log(body-size) on the x-axis and log(abundance) on the y-axis, while c) the size-
562 abundance pyramid shows log(abundance) on the x-axis and log(body-size) on the y-axis. Note
563 that the area A is the same in both panels. We use the community size-structure representation
564 throughout the paper as it facilitates comparisons between theory and experimental data, but see
565 Fig. 6 for a synthesis of our findings using the pyramid representation.

566

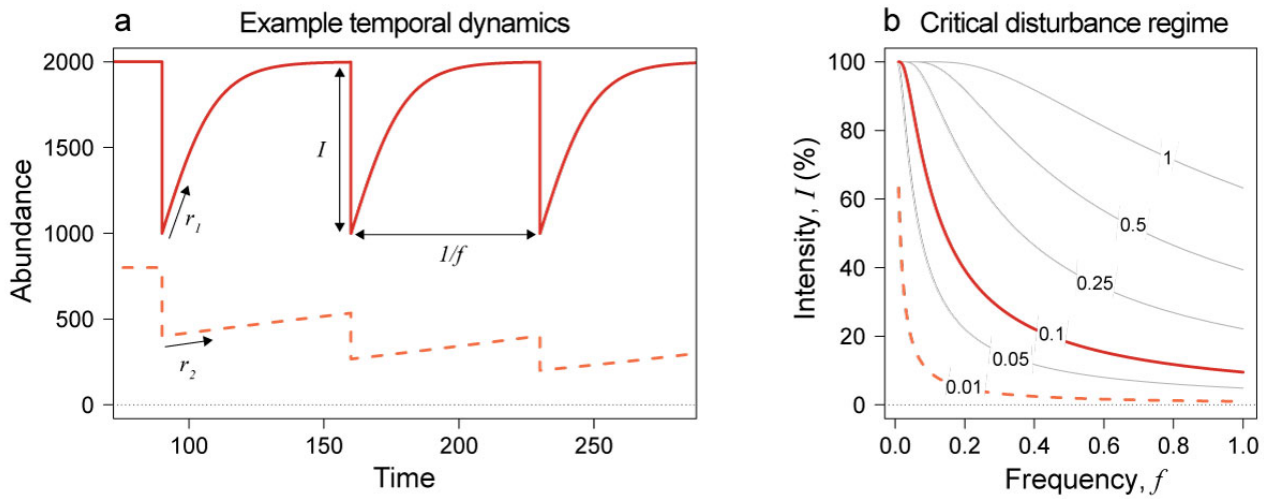

Figure 2: Population dynamics and persistence according to disturbance regime. a) Temporal dynamics of two species experiencing the same disturbance regime. Species 1 has a smaller body-size and therefore a higher growth rate than species 2. A population can persist only if its growth rate balances the long-term effect of the disturbance regime. We derive in equation (4) the mean abundance at dynamical equilibrium (i.e. temporal mean) of the persisting species experiencing varying disturbance regimes. b) Isoclines of the persistence criterion in the disturbance regime landscape according to population growth rate (numbers): on and above the line, the population of a given growth rate goes extinct. Lines with the same color code as in panel (a) correspond to the same growth rate.

578

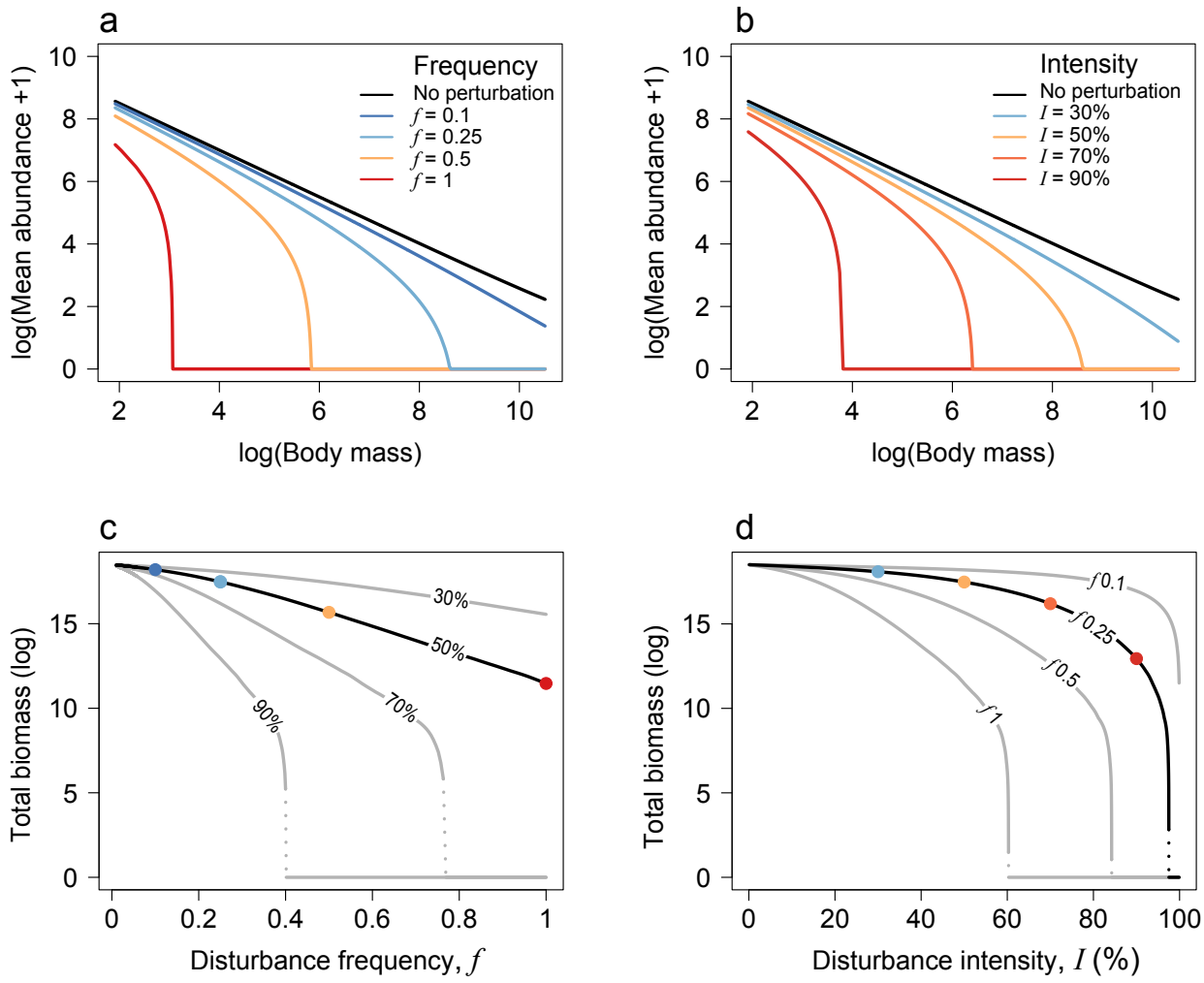

579

580 **Figure 3:** Effects of disturbance frequency and intensity on community size-structure and average
581 total biomass at dynamical steady state. Analytical results derived from Equation (5). a) Effect of
582 disturbance frequency (disturbance intensity is fixed to 50% abundance reduction), and b)
583 disturbance intensity (disturbance frequency is fixed to 0.25) on community size-structure. c)
584 Effect of disturbance frequency and d) intensity on average total biomass (in log), for different
585 intensities (c) and frequencies (d), respectively. Points on the black lines in (c) and (d) show the
586 disturbance regimes corresponding to community size-structures of the respective colors displayed
587 in panels (a) and (b).

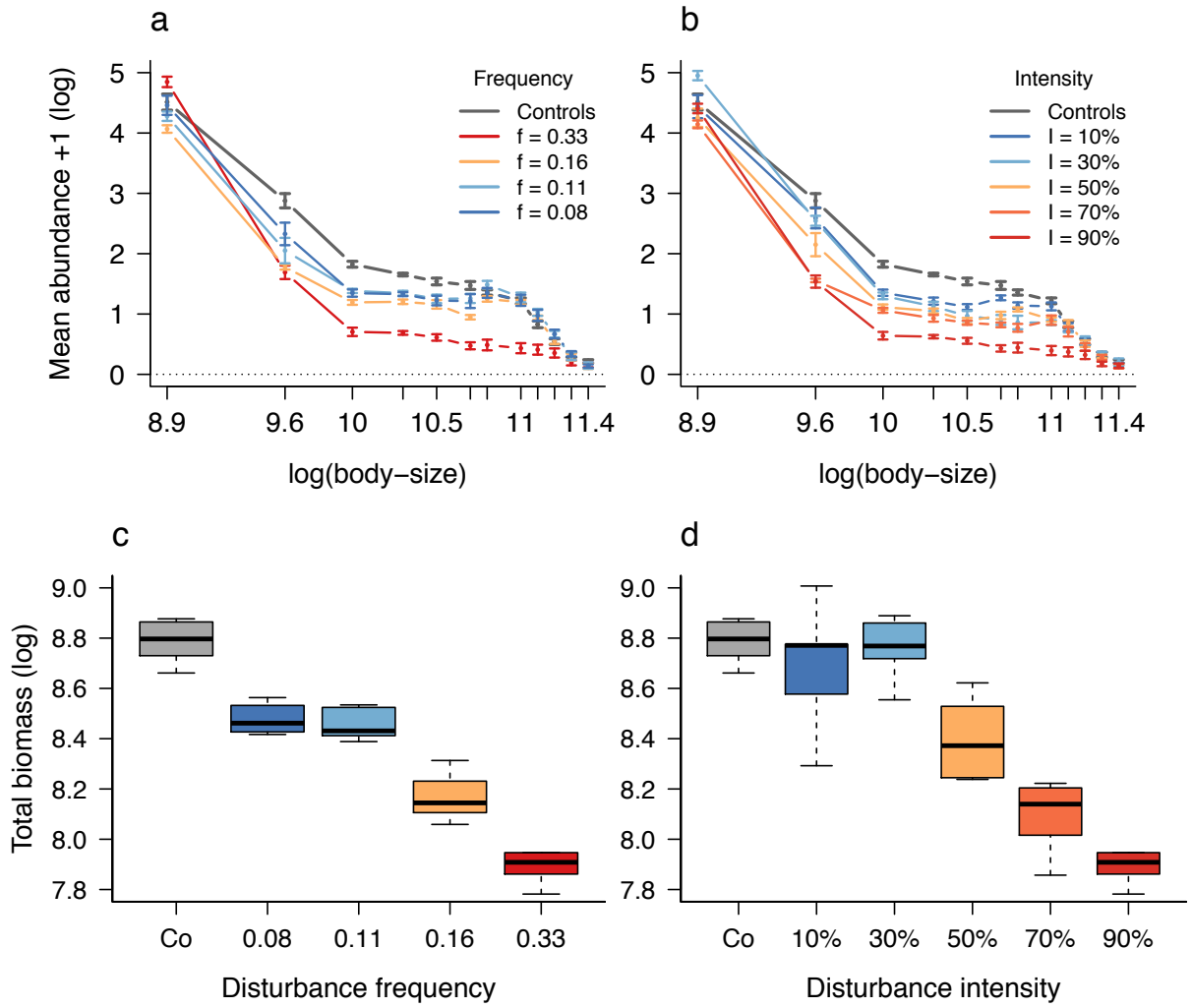

588

589

590 **Figure 4:** Experimental results. a) Effect of disturbance frequency on community size-structure.
591 Vertical bars illustrate mean abundance (individuals/µl) and its standard deviation over 21 time
592 points and 6 replicates for each size-class (µm^2). Disturbance intensity is fixed to I = 90%; other
593 intensities are shown in Fig. S2 and statistics in Table S2. b) Effect of disturbance intensity on
594 community size-structure. Disturbance frequency is fixed to f = 0.33, other frequencies are
595 shown in Fig. S3 and statistics in Table S2. Controls are in grey (undisturbed environment) and
596 axes are on a logarithmic scale. c) Effect of disturbance frequency on total community biomass
597 (temporal mean, n = 6 for treatments, n = 8 for controls, in µm^2/µl). Disturbance intensity is fixed

598 to I = 90% as in panel (a); other intensities are shown in Fig. S2. All frequencies have a
599 significant negative effect on total biomass compared to controls: Welch two sample t-tests: $f_{0.08}$:
600 t = 8, p-value < 0.001, $f_{0.11}$: t = 8.5, p-value < 0.001, $f_{0.16}$: t = 13.2, p-value < 0.001, $f_{0.33}$: t = 14.2,
601 p-value < 0.001. d) Effect of disturbance intensity on total community biomass (temporal mean, n
602 = 6 for treatments, n = 8 for controls, in $\mu m^2/\mu l$). Disturbance frequency is fixed to f = 0.33 as in
603 panel (b); other frequencies are shown in Fig. S3. All intensities except I = 10% and 30% have a
604 significant negative effect on total biomass compared to controls: $I_{10\%}$: t = 0.75, p-value = 0.48,
605 $I_{30\%}$: t = 0.5, p-value = 0.63, $I_{50\%}$: t = 6.1, p-value < 0.001, $I_{70\%}$: t = 12.7, p-value < 0.001, $I_{90\%}$: t =
606 14.2, p-value < 0.001.
607

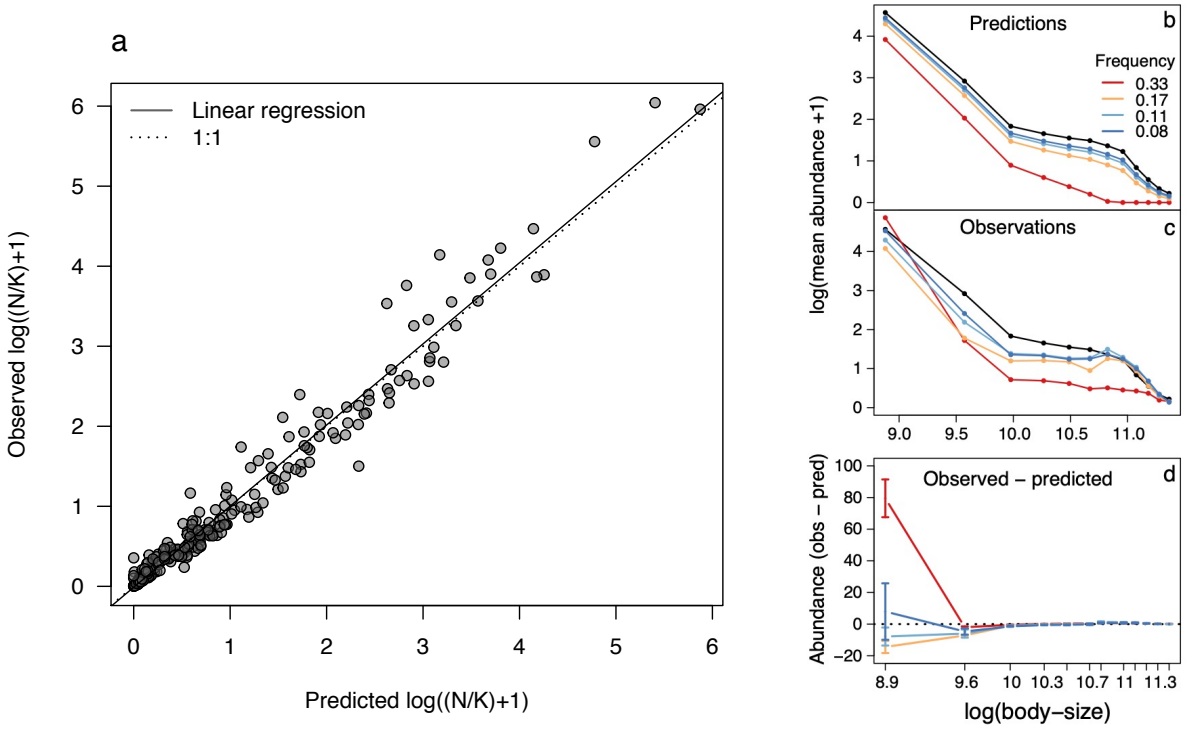

Figure 5: Comparison between experimental results and model predictions. a) Predicted vs. observed mean abundance *N* relative to carrying capacity *K* in the twelve size-classes for all the disturbance regimes (n=240). Solid line: linear regression [y = -0.012 + 1.01x, R^2 = 0.96, p-value < 0.001. Standard error for slope: 0.01, intercept: 0.02]. Dashed line indicates a 1:1 relationship. b) Predicted effect of disturbance frequency on the community size-structure of experimental communities. Disturbance intensity is fixed to *I* = 90%; other disturbance regimes are shown in Figs. S4-S5. Controls are in black (undisturbed environment) and axes are on a logarithmic scale. c) Observed effect of disturbance frequency on the community size-structure of experimental communities (similar to Fig. 4a). d) Difference between observed and predicted mean abundance for each size-class.

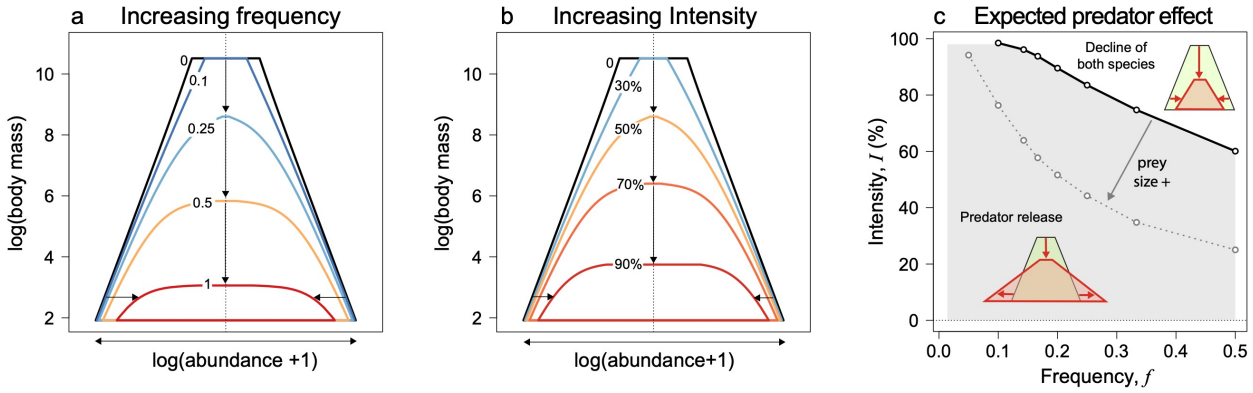

620

621

622 **Figure 6: Graphical summary of the effects of disturbances on the shape of size-abundance**
623 **pyramids.** Panels (a) and (b) show size-abundance pyramids for increasing disturbance frequency
624 and intensity, respectively (same analytical results as in Fig. 3a-b). Panel (c) illustrates the expected
625 change in the shape of size-abundance pyramids resulting from a predator-prey dynamic. Lines and
626 points in panel (c) represent isoclines of disturbance regimes $\{I, T\}$ under which we can expect a
627 predation-release effect leading to wider bases of size-abundance pyramids. Points represent the
628 disturbance intensity for which prey species switch from higher to lower mean abundances at
629 dynamical equilibrium in presence compared to in absence of disturbances, for a given disturbance
630 frequency and a set of predator parameters. Black points are estimated for a smaller prey, i.e. with
631 higher growth rate, than grey points (see detailed method in Appendix 3 and Table S4 for parameter
632 values).

633

634

Supporting Information

How pulse disturbances shape size-abundance pyramids

Claire Jacquet[1,2*], Isabelle Gounand[1,2], Florian Altermatt[1,2]

[1] Department of Aquatic Ecology, Swiss Federal Institute of Aquatic Science and Technology, Eawag, Dübendorf, Switzerland

[2] Department of Evolutionary Biology and Environmental Studies, University of Zurich, Zürich, Switzerland

* corresponding author: Claire.jacquet@eawag.ch.

Contents

6. Supplementary Figures

7. Supplementary References

1. Appendix 1: Analytical derivation of population mean abundance

To investigate the change in community size-structure with disturbances, we derive analytically the equilibrium mean abundance, $\overline{N}$, of a model in which a population displaying a logistic growth is submitted to recurrent pulse disturbances affecting all species in a similar way. This simple model is described in the methods section (see Fig. 2). The minimal abundance at equilibrium, N_{-}, that is the abundance just after a disturbance, is provided in Harvey *et al.* (2016), and gives, after simplification:

$$N_{-} = K\left(1 - \frac{I}{1 - e^{-rT}}\right) \quad (6)$$

with r and K the growth rate and the carrying capacity of the population, respectively. I and T are the intensity (proportion of abundance reduction) and the period (inverse frequency) of the disturbance regime, respectively.

To get the mean abundance, $\overline{N}$, we calculate the integral of the abundances between two disturbances at equilibrium, that is between 0 and T, the period of the disturbance regime:

$$\overline{N} = \frac{1}{T}\int_0^T f(t)dt \quad (7)$$

Here, the function $f(t)$ is the logistic solution, with t the time and N_0 the initial abundance:

$$f(t) = \frac{K}{1 + \left(\frac{K}{N_0} - 1\right)e^{-rt}} \quad (8)$$

To calculate $\overline{N}$, we note that equation (7) is equivalent to:

$$\overline{N} = \frac{1}{T}\big(F(T) - F(0)\big) \quad (9)$$

where F(x) is a primitive of $f(t)$. It can be shown by calculating its derivative that the following function is a primitive of the logistic solution (8):

$$F(t) = \frac{K\ ln(K + N_0 e^{rt} - N_0)}{r} \quad (10)$$

In our case, N_0 is the minimal abundance after a disturbance at equilibrium, $N\_$. By replacing equation (6) in (10), and then equation (10) in (9), we obtain the following expression:

$$\bar{N} = K\left(\frac{ln(1-I)}{Tr} + 1\right) \quad (11)$$

Since we are interested into community size-structure, we want to express mean abundance in function of mean population body-size on a log scale. For that, we assume the following allometric log-linear relationship between growth rate, r, and mean body-size, M, in accordance with the metabolic theory of ecology (Brown *et al.* 2004; Savage *et al.* 2004):

$$ln(r) = a_r \ln(M) + b_r \quad (12)$$

With a_r and b_r being the slope and the intercept of this allometric relationship.

Abundance also scales with body-size on a logarithmic scale (Brown & Gillooly 2003; Brown *et al.* 2004), then we can assume for carrying capacity:

$$ln(K) = a_K \ln(M) + b_K \quad (13)$$

With a_K and b_K being the slope and the intercept of this second allometric relationship.

By replacing (12) and (13) into (11), we finally obtain:

$$ln(\bar{N}) = a_K \ln(M) + b_K + ln\left(\frac{ln(1-I)}{Te^{a_r \ln(M) + b_r}} + 1\right) \quad (14)$$

The formula is valid when the expression in parentheses in the right-hand term is positive, which corresponds to the persistence criteria given in equations (2) and (3) of the main text.

We focus here on pulse disturbances to compare the theoretical predictions with the experimental results. However, press disturbances would have similar effects on size-abundance pyramids. Indeed, if we consider a constant additional mortality rate m on the logistic growth, such that population dynamics are described by:

$$\frac{dN}{dt} = rN\left(1 - \frac{N}{K}\right) - mN \qquad (15)$$

Then the abundance at equilibrium is $\bar{N} = K\left(1 - \frac{m}{r}\right)$ and the critical growth rate is $r > m$. This result demonstrates that press disturbances that are not size-selective will also exclude the large, slow growing species.

2. Appendix 2: Detailed methods to produce the theoretical results

We consider a community made of different co-occurring species constrained by intraspecific competition only. The species populations grow according to logistic functions (equation (1)) with specific growth rates, *r* and carrying capacities *K*, and are submitted to disturbances which recurrently reduce population abundances (every *T* units of time, the period) by destructing a proportion *I* (the intensity) of all species populations.

Equations (2) and (3) of the main text give the analytical derivation of the critical growth rate above which a population can persist under a given disturbance regime (combination of *I* and *T*). This allows to predict the set of disturbance regimes that a population can sustain (Fig. 2b) according to its growth rate, as well as the minimum generation time ($1/r$) needed to maintain a viable population under a given disturbance regime (Fig. S1).

To analyze the changes in community size-structure driven by disturbance regimes, we consider a set of 1000 co-occurring species, which body-sizes are randomly drawn from a lognormal distribution of mean 6 and standard deviation 1.5. This provides a range of sizes between 2 and 10 on a logarithmic scale. In an aquatic community for instance, it could correspond to a set of species from bacteria to planktivorous ranging from sizes of 5 µm to 22 mm. We assume a negative allometric relationship between growth rate and body-size (equation 12) with $a_r = -0.25$, a widely observed value for multiple taxa (Brown *et al.* 2004), and $b_r = 0.4$, a value which makes our growth rate gradient ranging approximately from 0.1 to 1, corresponding to common values for microorganisms when day is the time unit. We also derive the carrying capacity *K* of each species from its body-size assuming a log-linear relationship (equation (13)), with the slope $a_K = -0.75$, following a commonly observed value (Brown & Gillooly 2003; Brown *et al.* 2004), and the intercept $b_K = 10$, chosen to have values from 10 to 5000 for *K*,

which are, for instance, common values for microorganisms in terms of number of individuals per µl. We then calculate the mean abundance at equilibrium, $\overline{N}$, for each species population using equation (14), for different disturbance regimes $\{I, T\}$, to produce Figs. 3a and 3b and the abundance pyramids in Figs. 6a and 6b (same values). In the figures, f corresponds to the disturbance frequency: $f = 1/T$. Parameter values are summarized in Table S1.

Then, we calculate community total biomass by summing the biomass of each of the 1000 species populations within the community, with species biomass, B, calculated as the product of mean abundance at equilibrium, $\overline{N}$, and the average individual body-size in the population, M:

$$B = \overline{N}M$$

We provide total biomass of the community for scenarios covering a whole landscape of disturbance regimes $\{I, T\}$ in Figs. 3c and 3d.

Addition of stochasticity in intensity and frequency of disturbances

The above analysis was first conducted for strictly regular disturbances of the same magnitude. We then investigate the effect of variability of disturbance period and intensity on the community size-structure. We run simulations of the same 1000 co-occurring species than previously but with sequences of disturbance periods and intensities drawn from a uniform distribution within an interval defined by a percentage of deviation from the mean (see Table S5). Results are robust to this variation for weak to relatively strong regimes of disturbances. For very high disturbance intensities and frequencies, the variability of disturbances characteristics increases by drift the extinction of the larger species (Figure S6). The effect is more pronounced for intensity variability, while for periods, increase in extinction occur only for very large variations around

already short periods (mean±100%). In that case, consecutive very short periods selected by chance can prevent recovery.

For instance, let's take the case shown in Fig. S6 in the top right panel, for which pulse disturbances were of mean intensity 80% with a variability of 25% (in terms of deviation from the mean) and a mean period of 3 days with a variability of 100%. This means that we created sequences of disturbances (one for each replicate simulation applied to all species of the community) with the intensity of each disturbance and the period between each pair of disturbances being randomly drawn from the intervals [60%,100%] and [0,6], respectively.

Sensitivity analyses

We consider that the allometric parameters of the relationships between population growth rate, carrying capacity and body-size are the same for all species (i.e. same slopes and intercepts). However, the intercepts can be variable between taxonomic groups (Brown *et al.* 2004). Moreover, while multicellular organisms have growth rates that scale with body-size with a slope of -1/4, a slope of -1 has been reported for unicellular organisms (DeLong *et al.* 2010). We therefore perform sensitivity analyses of Equation (5) to assess the robustness of our results to variation in these allometric parameters. Increasing the slope (toward more negative values) or decreasing the intercept of the relationship between population growth rate and body-size has the same qualitative impact on community size-structure: it decreases the size-specific criterion for population persistence (equation 3) and therefore truncates the community size-structure from its largest species (Fig. S7). Small species are not impacted by changes in the slope, except when disturbances are very strong. Finally, the slope and intercept of the allometric relationship between carrying capacity and body-size essentially change the steepness of a pyramid's sides, but not their qualitative response to disturbances (Fig. S8). Note that this slope is modulated by

additional variables in multitrophic communities, namely predator-prey mass ratio and predator trophic efficiency (Jennings & Mackinson 2003; Blanchard *et al.* 2009; Trebilco *et al.* 2013). A further step will be to integrate these variables into the model to capture the effect of disturbances on the size-structure of multitrophic communities.

3. Appendix 3: Predator-prey model and interaction-release effect

We focus here on the effect of predator-prey dynamics on the shape of size-abundance pyramids exposed to disturbances. We hypothesize that specific disturbance regimes could trigger a predation release after a disturbance event that would allow small, fast-growing prey species to reach higher abundances compared to the undisturbed case. We investigate this hypothesis using a Lotka-Volterra predator-prey model, where the dynamics of prey and predator abundances, N and P, are described by the following system of differential equations:

$$\frac{dN}{dt} = \left(1 - \frac{N}{K}\right) rN - aPN \quad (15)$$

$$\frac{dP}{dt} = (a\varepsilon N - m)P \quad (16)$$

with K and r the carrying capacity and the intrinsic growth rate of the prey, respectively, and ε, a, and m the conversion efficiency, attack and mortality rates of the predator, respectively. We added recurrent disturbances to this dynamic as described in the previous section.

We examine the effects of recurrent pulse disturbances on a predator-prey system by means of simulations (see Table S6 for parameter values). To avoid issues arising from synchrony between intrinsic oscillations of the system and disturbance regime, species parameters are chosen to have stable equilibrium for the case without disturbance, and simulations start with species abundances set to their equilibrium without disturbances, which are easily derived analytically. After 1000 units of time, disturbances start and dynamics are run until 50,000 units of time, which was sufficient to reach equilibrium in the parameter space explored. Dynamics are calculated in a C++ code (see html file). For numerical integration, we use an adaptive step solver provided in the GNU Scientific Library, GSL version 2.5 (Galassi et al. 2011), using the Runge-Kutta Kash-Carp method. We estimate mean abundances at equilibrium by averaging prey or predator abundances over ten disturbance periods (time between eleven disturbances).

We hypothesize that specific disturbance regimes could trigger a transient predation release after a disturbance event that would allow small, fast-growing prey species to reach higher abundances compared to the undisturbed case. To test this hypothesis, we focus on how change in disturbance regime modulates the equilibrium abundance of a specific predator-prey system. Predator parameters are chosen to have prey abundance without disturbance of 100 individuals per area unit (see Tables S4 and S6). As we are also interested into understanding if faster prey benefit from a higher predation release effect, we vary prey body-size, and thus prey growth rate through equation (12), while keeping predator parameters constant (this is equivalent to varying the predator-prey size ratio). We choose prey carrying capacity such that the predator persists for a wide range of disturbance regimes, but eventually goes extinct in too harsh disturbance regimes. Figs. S9 to S11 show the results for an extended parameter space of disturbance regimes and prey body-sizes (see Table S6 for parameter values).

Finally, we are interested in linking this result to change in the shape of size-abundance pyramids. For that, we summarize the results of the predation-release effect for two prey body-sizes in Fig. 6c. Overall, disturbances always have a positive effect on prey abundance for low to intermediate disturbances regimes. Then, when increasing the strength of disturbances, a case happens for which disturbances are so strong that prey mean abundance is also negatively affected. We determine the critical disturbance intensity for which prey mean abundance drops below the case without disturbances for a given disturbance period (or frequency). For that, we run a set of simulations with a small increment of disturbance intensity (see Table S4) and estimate this threshold via a linear approximation between the two closest points to the threshold (see provided code). Under the isoclines representing the threshold intensity for different disturbance frequencies, the predator-release effect operates and is stronger than the negative impact of disturbances on prey species. In that case we might observe a widening of abundance

pyramid' bases with disturbance in trophic communities (Fig. 6c). Larger prey sizes (or lower predator-prey size ratio) bring down the predator-release isocline to weaker disturbance regimes, reducing the disturbance regime space in which disturbance might lead to pyramids with wider bases.

Code release

We will release the code through a Rmarkdown document and an associated C++ source code file. We thank the developers of R version 3.6.1 (R Core Team 2019), Rmarkdown, and those of the R-C++ interface, that we used in the script. Specifically, we used R version 3.5.1 and the following R-packages: "***Rcpp***" version 1.0.0 (Eddelbuettel and Francois 2011, Eddelbuettel 2013, Eddelbuettel and Balamuta 2017), and "***RcppGSL***" version 0.3.6 (Eddelbuettel and Francois 2018). "Rmisc" version 1.5 (Hope 2013) has been used to calculate confidence intervals in Figure S6.

4. Appendix 4: Full experimental methods

We conducted an experiment in aquatic microcosms inoculated with 13 protist species *(Blepharisma* sp.*, Cephalodella* sp. *Chilomonas* sp.*, Chlorogonium euchlorum, Colpidium* sp., *Cyclidium* sp.*, Euglena gracilis, Euplotes aediculatus, Loxocephalus* sp.*, Paramecium aurelia, Paramecium caudatum, Spirostomum* sp. and *Tetrahymena* sp.) and a set of common freshwater bacteria (*Serratia fonticola*, *Bacillus subtilis* and *Brevibacillus brevis*) as a food resource. These protist species cover a wide range of body-sizes (from 10–10^3 microns) and densities (10–10^5 individuals/ml, Giometto *et al.* 2013). All species are bacterivores whereas three of them can also photosynthesize and two species can feed on smaller protists (Table S7). General lab procedures follow the protocols described in (Altermatt *et al.* 2015). The microcosms consisted of a 250 ml Schott bottle filled to 100 ml. They were assembled by first filling each Schott bottle with 30 ml of pre-autoclaved standard protist medium (Carolina Biological Supply, Burlington NC, USA), and 5 ml of a bacteria solution. After 24 h, to allow time for bacteria growth, we added 65 ml of protist solution mixing 5 ml of each protist species at carrying capacity. All communities were allowed to grow for one week before disturbance treatments started.

Experimental design

We performed a factorial experiment in which we varied disturbance frequency and intensity, resulting in a total of twenty different disturbance regimes. Disturbance was achieved by boiling a fraction of the well-mixed community in a microwave. We let the medium cool down before putting it back into the microcosm. This procedure allowed to keep the composition of the microcosm constant and to avoid nutrient addition or loss. It mimics disturbances such as fire and flooding, that initially reduce population abundance but may also enhance the regeneration of

nutrients (Haddad *et al.* 2008). Disturbance intensities ranged from 10, 30, 50, 70 to 90%. We disturbed microcosms at four frequencies: f = 0.08, 0.11, 0.16 and 0.33, corresponding to a disturbance every 12, 9, 6 and 3 days respectively. The experiment lasted for 21 days, or 10–50 generations depending on species. Each disturbance regime was replicated six times. To control for the intrinsic variability of abundance pyramids, we cultured eight undisturbed microcosms under the same conditions.

Sampling

We sampled 0.2 ml of each microcosm daily to quantify individual body-sizes (i.e. mean cell area in μm^2), protist abundances (individuals/µl) and total community biomass (i.e. total bioarea in μm^2/µl) using a standardized video procedure (Altermatt *et al.* 2015; Pennekamp et al. 2017). A constant volume (14.9 µl) of each sample was placed under a dissecting microscope connected to a camera and a computer for the recording of videos (4 seconds per video). Then, using image processing software (IMAGEJ, National Institute of Health, USA) and the R-package *bemovi* (Pennekamp *et al.* 2015) we extracted the number of moving organisms per video frame and the size of each individual (mean cell area in μm^2). We estimate total biomass as the sum area of all individuals averaged by video frames, assuming proportionality between area and mass. Other traits such as organisms' speed and shape were used to filter out background movement noise (e.g. particles from the medium).

Statistical analyses

We binned the observed individuals into twelve size-classes ranging from 0 to 1.6×10^5 μm^2 in order to get statistically comparable community size-structures. The mean abundance and its standard

deviation in each size-class were calculated over 21 time points and 6 replicates (total of 126 observations) for each treatment and over 21 time points and 8 replicates (total of 168 observations) for the control communities. We performed Welch two sample t-tests of mean comparison (treatment versus control) to determine which disturbance regime had a significant effect on community size-structure and total community biomass. Results are presented in Table S2, Fig.4, Fig. S2 and Fig. S3.

5. Supplementary Tables

Table S1: Model parameters for the results showed in Fig. 3.

Symbol	Definition	Values	Dimension	Comments
μ_{size}	Mean of the log-normal distribution of community body-size	6	L	
σ_{size}	Standard deviation of the log-normal distribution of community body-size	1.5	L	
a_r	Slope of the relationship between body-size and growth rate in a log space	-0.25	$T^{-1}L^{-1}$	Brown et al 2004
b_r	Intercept of the relationship between body-size and growth rate in a log space	0.4	T^{-1}	
a_K	Slope of the relationship between body-size and carrying capacity in a log space	-0.75	$L^{-2}L^{-1}$	Brown et al 2004
b_K	Intercept of the relationship between body-size and carrying capacity in a log space	10	L^{-2}	Log number of individuals per area
I	Disturbance intensity	0.001–0.999	ø	Proportion of punctual abundance reduction
T	Disturbance period	1–100	T	Time between two disturbances

Dimensions L and T mean length and time, respectively.

Table S2: Statistics for the effect of all disturbance regimes on community size-structure. Effects of disturbance frequency $f = 1/T$ and intensity I on the community size-structures presented in Figs. 4, S2 and S3. Statistics of Welch two-sample t-tests of mean comparison (treatment versus control). Values in blue and red indicate a significant positive and negative effect of the disturbance regime on the mean abundance compared to controls, respectively (i.e., p-value ≤ 0.05). The twelve size-classes (S1 to S12) range from 0 to 1.6×10^5 µm^2 and all have a width of 1.4×10^4 µm^2.

		Size-classes (from the smallest to the largest)											
I	***f***	**S1**	**S2**	**S3**	**S4**	**S5**	**S6**	**S7**	**S8**	**S9**	**S10**	**S11**	**S12**
10%	0.33	-1.7	0	**4.9**	**6.9**	**4.5**	1.5	1.1	-0.3	-0.4	-0.6	-0.5	0.9
10%	0.16	0.9	**2.5**	1.2	**4**	1.1	1.7	-0.3	-0.5	-1.4	-0.4	0.6	0.6
10%	0.11	-1	-0.8	1.7	0.6	0.7	-0.1	-0.7	0.8	0.6	1.3	0.4	1.2
10%	0.08	0.7	1.8	**2.9**	**5.2**	2	2.1	1.4	**2.7**	0.7	1.2	1	1.2
30%	0.33	**-6.1**	0.8	**5.7**	**5.7**	**5.3**	**4.3**	**2.8**	**3.8**	-0.2	-1.1	-0.9	-0.1
30%	0.16	-0.6	0.7	2.1	1.7	**3.9**	**3.6**	1.8	1.8	-1.8	0	0	1.6
30%	0.11	-1.6	0.7	2.2	**2.4**	**2.5**	2.1	0.4	-0.9	-1.6	0	0.2	1.1
30%	0.08	-1.6	-0.9	**2.8**	2.4	1.9	**3.5**	1.3	0.5	-0.7	0	0.3	0
50%	0.33	-0.8	2.1	**8.6**	**11.1**	**7.3**	**4.6**	**3.1**	**3.7**	-1	-0.3	0.6	1.6
50%	0.16	**-2.7**	1.4	**3.8**	**5.5**	**4.4**	**4.3**	**2.8**	1.1	-1.2	-0.8	-0.4	2.1
50%	0.11	-1.6	-0.7	**3.9**	**7**	**2.6**	**2.6**	-0.5	-0.5	**-2.8**	-2	-0.7	0.7
50%	0.08	-0.3	1.8	**2.6**	**3.4**	**5.2**	**3.8**	2	-0.2	-1.3	-1.7	0	**2.6**
70%	0.33	0.1	**6.7**	**10.5**	**9.2**	**7.5**	**6.6**	**6.3**	**2.7**	0.2	1.1	1	1.5
70%	0.16	-2.1	**3.3**	**5.5**	**5.2**	**3**	**2.7**	0.7	-0.3	-1.5	-0.7	1.3	0.3
70%	0.11	**-2.5**	-0.3	**6**	**8.9**	**5.6**	**4.3**	**2.6**	1.5	-1.3	-0.4	0.6	1.5
70%	0.08	-0.9	**2.7**	**3.8**	**2.7**	**3.8**	**3.5**	1	1.2	-1.4	-0.7	-0.1	0.4
90%	0.33	-1.7	**6.3**	**10.4**	**17.6**	**9.8**	**9.8**	**9**	**7.3**	**4.3**	**2.9**	**2.8**	1.1
90%	0.16	**3.6**	**6.6**	**8.4**	**10.2**	**4.7**	**6.4**	1.6	-0.1	-2.2	-0.5	0.4	1.6
90%	0.11	1.8	**2.9**	**6.8**	**6.8**	**3.4**	2.3	-1.9	-0.8	**-2.8**	-1.7	0.1	0.9
90%	0.08	0.7	**2.6**	**5.9**	**9.7**	**3.5**	1.7	-0.3	-0.4	-1.6	-1.4	-0.4	1.8

Table S3: Model parameters for the results showed in Fig. 5.

Symbol	Definition	Values	Units	Comments
a_r	Slope of the relationship between body-size and growth rate in a log space	-0.37	$\log(\mu m^2)^{-1}$ $\log(d^{-1})$	From experimental data
b_r	Intercept of the relationship between body-size and growth rate in a log space	3.75	$\log(d^{-1})$	From experimental data
M	Midpoints of size-classes (cell area)	7,182–86,185	μm^2	From experimental data
K	Carrying capacities per size-class	244–95,387	individuals/µl	From experimental data
I	Disturbance intensity	0.1–0.9	ø	Proportion of punctual abundance reduction
T	Disturbance period	3–12	d	Time between two disturbances

Table S4: Predator-prey model parameters for the simulations showed in Fig. 6c.

Symbol	Definition	Values	Dimension	Comments
M	Prey body-size	100, 10000	L	
a_r	Slope of the relationship between body-size and growth rate in a log space	-0.25	$T^{-1}L^{-1}$	Brown et al 2004
b_r	Intercept of the relationship between body-size and growth rate in a log space	0.4	T^{-1}	
K	Prey carrying capacity	5000	L^{-2}	number of individuals per area
a	Predator attack rate	0.01	T^{-1}/L^{-2}	attacks per predator (given their abundance per area) and per unit of time
m	Predator mortality rate	0.1	T^{-1}	Proportion of predator death per unit of time
ε	Predator conversion efficiency	0.1	ø	Proportion of prey caught converted into predator
I	Disturbance intensity (in %)	0 to 99.9 by increment of 0.1	ø	Percentage of punctual abundance reduction
T	Disturbance period	2, 3, 4, 5, 6, 7, 10, 20, 100	T	Time between two disturbances

Dimensions L and T mean length and time, respectively.

Table S5: Model parameters for the results showed in Fig. S6.

Symbol	Definition	Values	Dimension	Comments
μ_{size}	Mean of the log-normal distribution of community body-size	6	L	
σ_{size}	Standard deviation of the log-normal distribution of community body-size	1.5	L	
a_r	Slope of the relationship between body-size and growth rate in a log space	-0.25	$T^{-1}L^{-1}$	Brown et al 2004
b_r	Intercept of the relationship between body-size and growth rate in a log space	0.4	T^{-1}	
a_K	Slope of the relationship between body-size and carrying capacity in a log space	-0.75	$L^{-2}L^{-1}$	Brown et al 2004
b_K	Intercept of the relationship between body-size and carrying capacity in a log space	10	L^{-2}	Log number of individuals per area
I	Disturbance intensity	0.8	ø	Proportion of punctual abundance reduction
T	Disturbance period	3	T	Time between two disturbances
dev_I	Deviation from mean intensity defining the interval of the uniform distribution from which variable intensities are drawn	0, 10, 20, 25	%	Percentage
dev_T	Deviation from mean period defining the interval of the uniform distribution from which variable periods are drawn	0, 25, 50, 100	%	Percentage
$tmax$	Maximum time of the simulations	10,000	T	
h	Time step	0.01	T	
rep	Number of replicate disturbance sequences	100	ø	

Dimensions L and T mean length and time, respectively.

Note: Lower disturbance intensities ($I \in \{0.3,0.5,0.6\}$) and longer periods ($T \in \{5,10,50\}$) have been explored, resulting in lower effects of variability than those shown in Fig. S8

Table S6: Predator-prey model parameters for the simulations showed in Figs. S9-S11.

Symbol	Definition	Values	Dimension	Comments
M	Prey body-size	10, 30, 100, 300, 1000, 3000, 10000	L	
a_r	Slope of the relationship between body-size and growth rate in a log space	-0.25	$T^{-1}L^{-1}$	Brown et al 2004
b_r	Intercept of the relationship between body-size and growth rate in a log space	0.4	T^{-1}	
K	Prey carrying capacity	5000	L^{-2}	number of individuals per area
a	Predator attack rate	0.01	T^{-1}/L^{-2}	attacks per predator (given their abundance per area) and per unit of time
m	Predator mortality rate	0.1	T^{-1}	Proportion of predator death per unit of time
ε	Predator conversion efficiency	0.1	ø	Proportion of prey caught converted into predator
I	Disturbance intensity (in %)	0, 10, 20, 30, 40, 50, 60, 70, 80, 90, 95	ø	Percentage of punctual abundance reduction
T	Disturbance period	0, 2, 3, 4, 5, 8, 10, 20, 100	T	Time between two disturbances

Dimensions L and T mean length and time, respectively.

Table S7: Species information. Species names, taxonomic group, average length (μm), carrying capacity *K* (individuals/ μl), growth rate *r* (1/day) and trophic status (bacterivores, autotroph, predators). Species' traits (mean ± SD) are from Carrara *et al.* (2012), Haddad *et al.* (2008) and lab measurements.

Species	Taxonomic group	Length (μm)	K (ind/ml)	r (1/d)	Feeding type
Blepharisma sp.,	Ciliate	471.3 ± 57.1	59.5 ± 4.7	0.67 ± 0.07	Bact/predator
Cephalodella sp.	Rotifer	112.7 ± 11.2	902.8 ± 121.8	0.67 ± 0.11	Bact
Chilomonas sp.,	Flagellate	23.3 ± 3.7	1572 ± 278.3	0.98 ± 0.13	Bact
Chlorogonium euchlorum	Flagellate	30	-	-	Bact/autotroph
Colpidium sp.,	Ciliate	81 ± 7.8	1379 ± 76.6	1.5 ± 0.08	Bact
Cyclidium sp.	Ciliate	20	4038	1.51	Bact
Euglena gracilis	Flagellate	36.7 ± 6.4	84 578	0.87	Bact/autotroph
Euplotes aediculatus	Ciliate	85.4 ± 8.6	359	0.43	Bact/autotroph
Loxocephalus sp.	Ciliate	140	-	-	Bact
Paramecium aurelia	Ciliate	111.6 ± 15.1	111.1± 2.6	0.86 ± 0.02	Bact
Paramecium caudatum	Ciliate	250	-	-	Bact
Spirostomum sp.	Ciliate	843.8 ± 149.7	13.6 ± 4.2	0.57 ± 0.15	Bact/predator
Tetrahymena sp.	Ciliate	26.7 ± 4.8	2997 ± 196	2.24 ± 0.15	Bact

6. Supplementary Figures

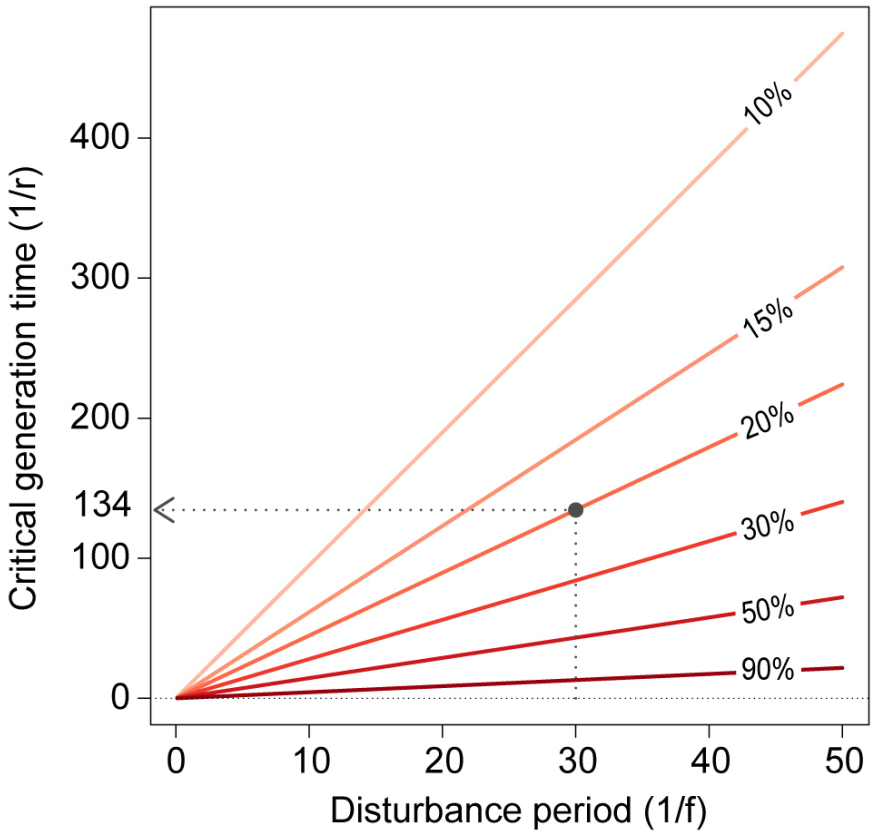

Figure S1: Critical generation time required for long-term population persistence under different disturbance regimes (equation (2)). Disturbance period is on the x-axis and the lines depict different disturbance intensities (percentage of abundance reduction). As an example, the grey point shows that if a population experiences a recurrent disturbance killing 20% of the population every 30 time units, it has to have a generation time (time needed to double the population) of less than 134 time units to persist.

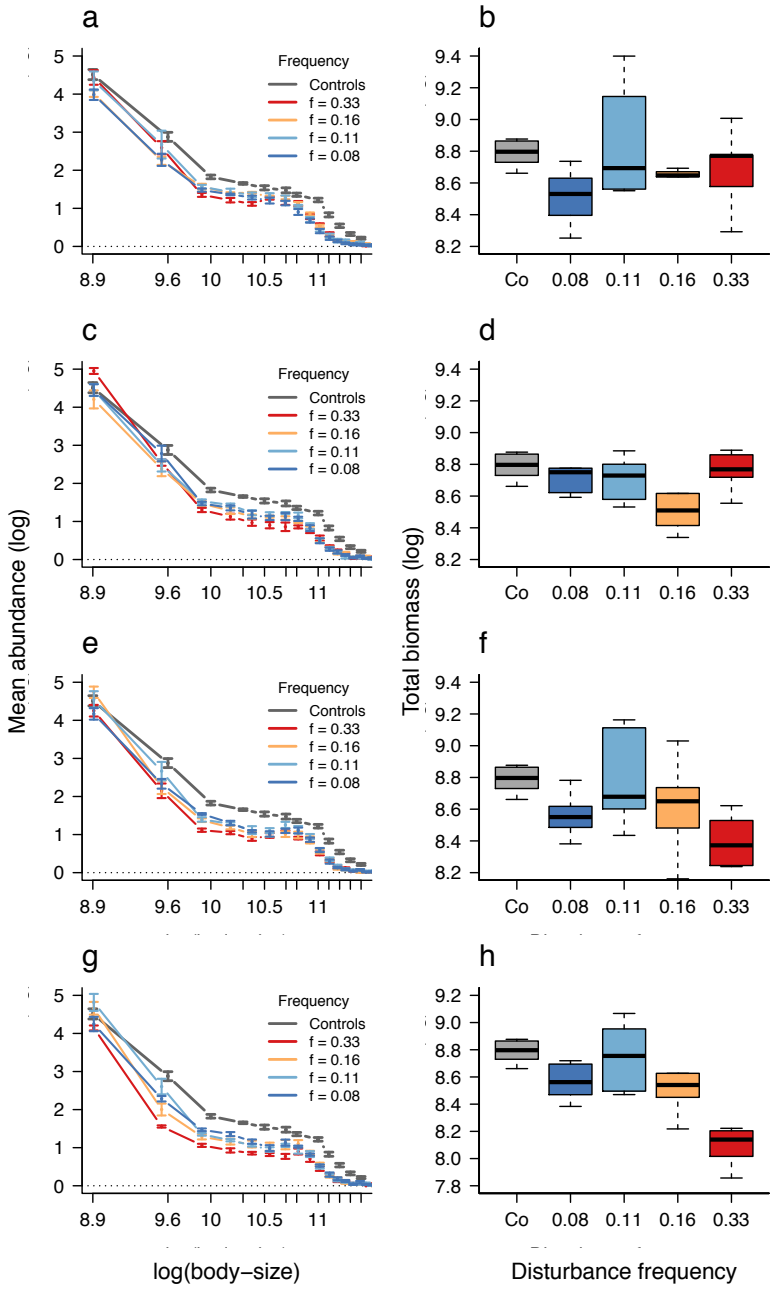

Figure S2: Effect of disturbance frequency on community size-structure and total biomass for different disturbance intensities: a-b) *I* = 10% c-d) *I* = 30%, e-f) *I* = 50%, g-h) *I* = 70%. See Fig. 5 for *I* = 90%. Statistics of the Welch two-sample t-tests for the effect of disturbance regimes on total biomass compared to controls: **b) *I* = 10%:** $f_{0.08}$: t = 3.95, p-value = 0.004, $f_{0.11}$: t = -0.62, p-value = 0.56, $f_{0.16}$: t = 4.15, p-value = 0.002, $f_{0.33}$: t = 0.75, p-value = 0.48). **d) *I* = 30%:** $f_{0.08}$: t = 0.24, p-value = 0.82, $f_{0.11}$: t = 1.22, p-value = 0.26, $f_{0.16}$: t = 1.7, p-value = 0.29, $f_{0.33}$: t = 0.5, p-value = 0.63). **f) *I* = 50%:** $f_{0.08}$: t = 3.74, p-value = 0.005, $f_{0.11}$: t = -0.17, p-value = 0.87, $f_{0.16}$: t = 1.26, p-value = 0.26, $f_{0.33}$: t = 6.15, p-value < 0.001. **h) *I* = 70%:** $f_{0.08}$: t = 3.82, p-value = 0.004, $f_{0.11}$: t = 0.12, p-value = 0.91, $f_{0.16}$: t = 1.5, p-value = 0.18, $f_{0.33}$: t = 12.7, p-value < 0.001). See Table S3 for the significance of each treatment on the size-classes of the community size-structure.

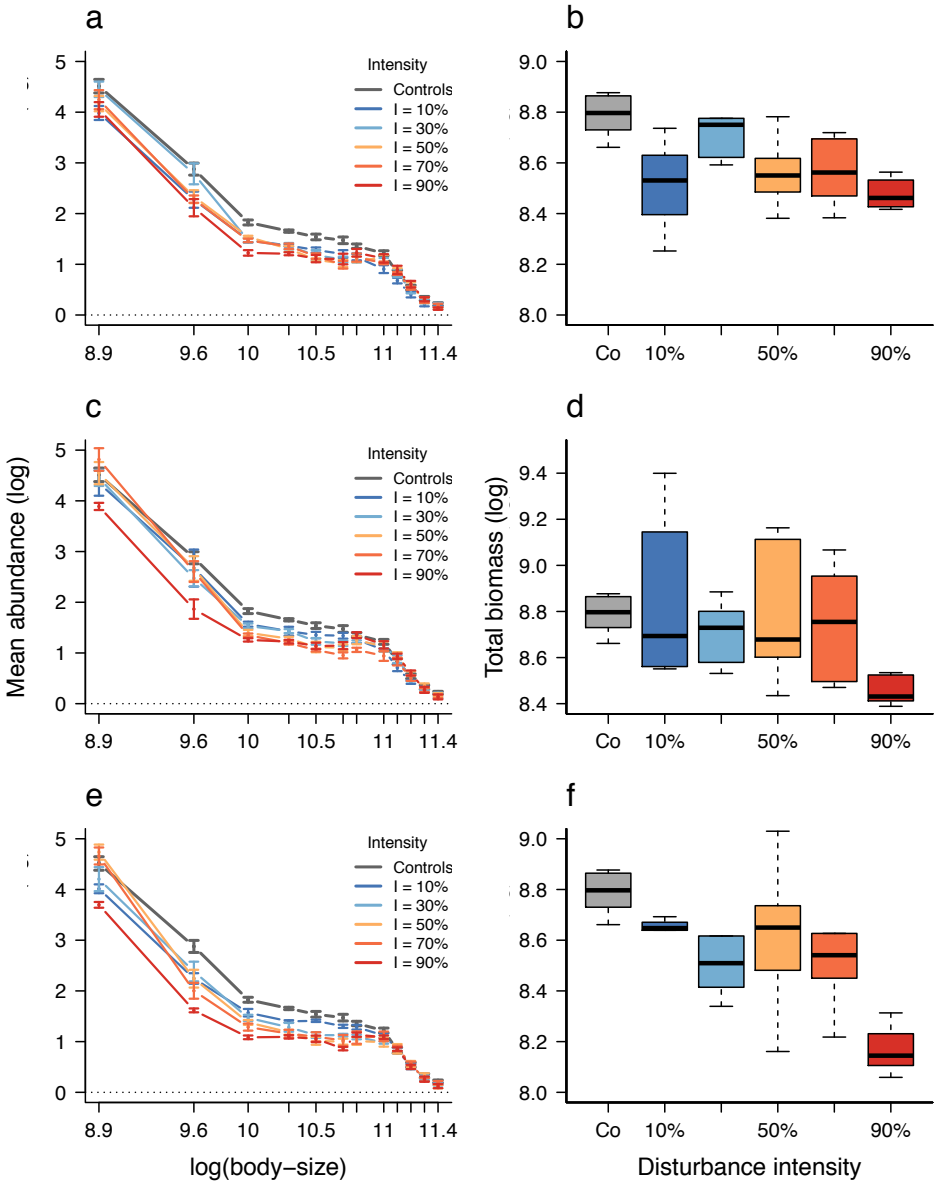

Figure S3: Experimental results: effect of disturbance intensity on community size-structure and total biomass for different disturbance frequencies: a-b) $f = 0.08$, c-d) $f = 0.11$, e-f) $f = 0.16$. See Fig. 5 for $f = 0.33$. Statistics of the Welch two-sample t-tests for the effect of disturbance regimes on total biomass compared to controls: **b) $f = 0.08$:** $I_{10\%}$: t = 4, p-value = 0.004, $I_{30\%}$: t = 0.2, p-value = 0.81, $I_{50\%}$: t = 3.7, p-value = 0.004, $I_{70\%}$: t = 3.8, p-value = 0.004, $I_{90\%}$: t = 8, p-value < 0.001. **d) $f = 0.11$:** $I_{10\%}$: t = -0.6, p-value = 0.56, $I_{30\%}$: t = 1.2, p-value = 0.25, $I_{50\%}$: t = -0.17, p-value = 0.87, $I_{70\%}$: t = 0.12, p-value = 0.9, $I_{90\%}$: t = 8.5, p-value < 0.001. **f) $f = 0.16$:** $I_{10\%}$: t = 4.1, p-value = 0.001, $I_{30\%}$: t = 1.17, p-value = 0.29, $I_{50\%}$: t = 1.26, p-value = 0.25, $I_{70\%}$: t = 1.5, p-value = 0.18, $I_{90\%}$: t = 13.2, p-value < 0.001. See Table S3 for the significance of each treatment on the size-classes of the community size-structure.

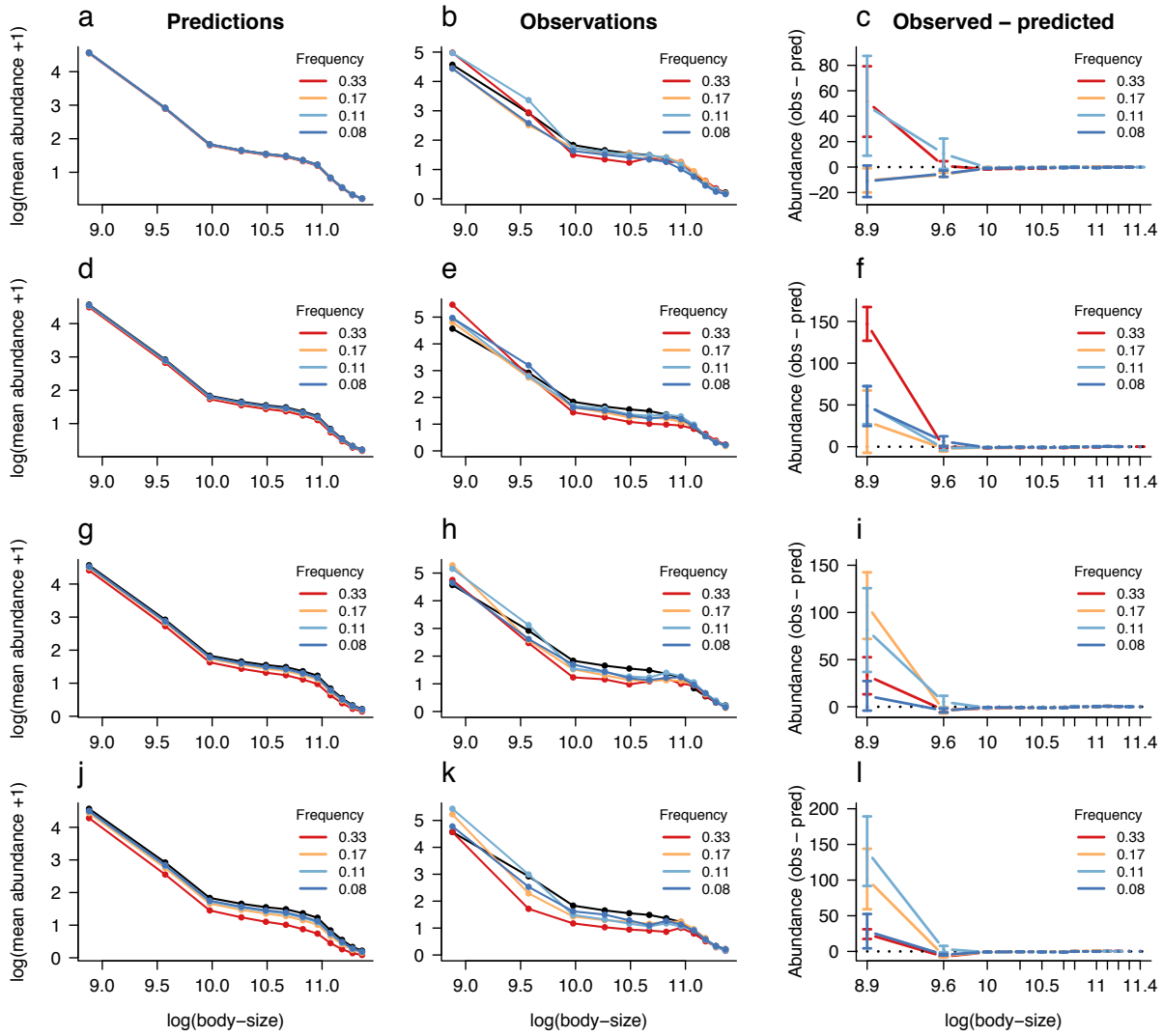

Figure S4: Comparison between experimental results and model predictions for different disturbance intensities: a-c) *I* = 10% d-f) *I* = 30%, g-i) *I* = 50%, j-l) *I* = 70%. a, d, g, j) Predicted effect of disturbance frequency on the community size-structure of experimental communities. b, e, h, k) Observed effect of disturbance frequency on the community size-structure of experimental communities (similar to Fig. 4a). c, f, i, l) Difference between observed and predicted mean abundance for each size-class.

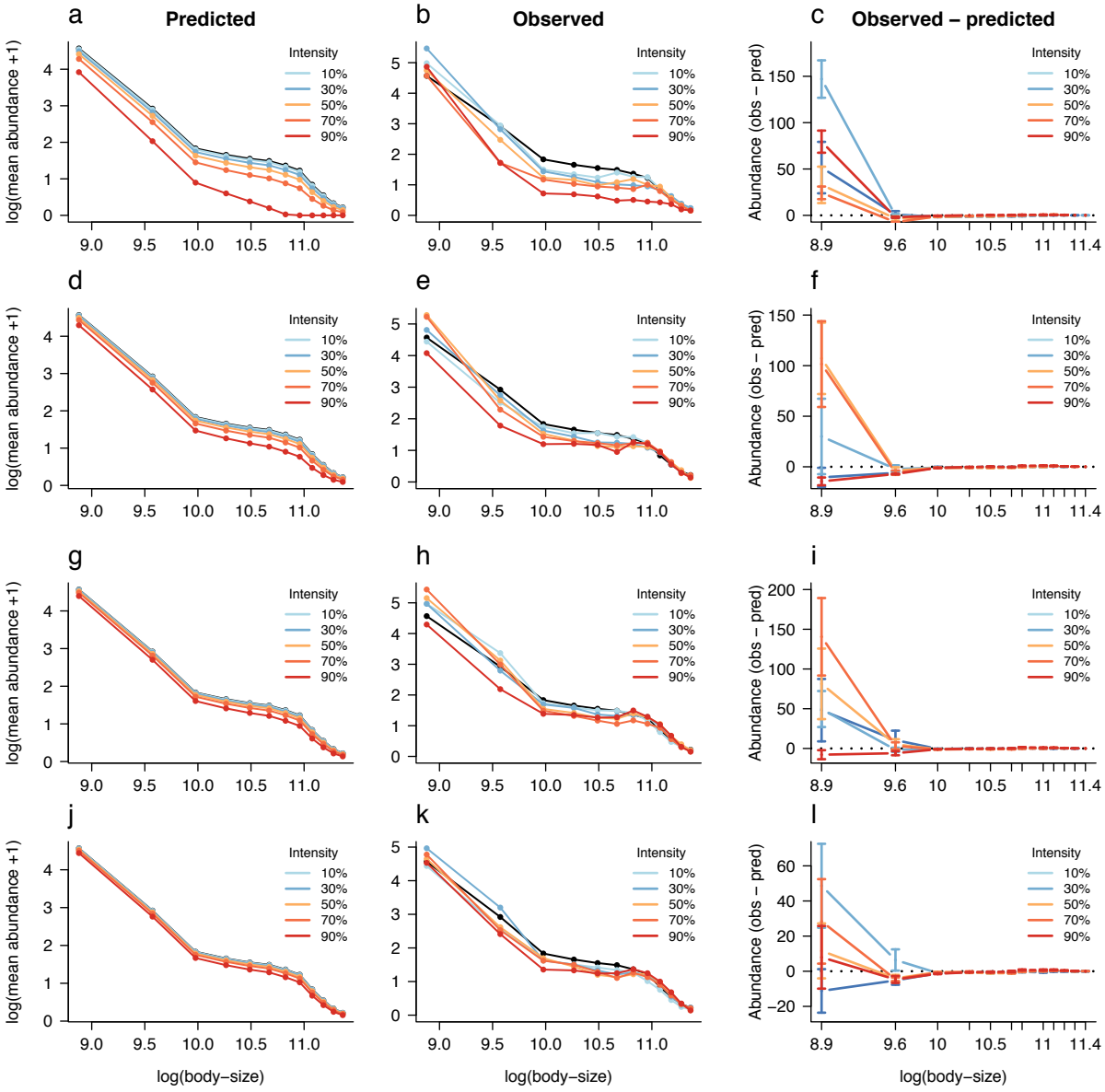

Figure S5: Comparison between experimental results and model predictions for different disturbance frequencies: a-c) $f = 0.33$ d-f) $f = 0.16$, g-i) $f = 0.11$, j-l) $f = 0.08$. a, d, g, j) Predicted effect of disturbance intensity on the community size-structure of experimental communities. b, e, h, k) Observed effect of disturbance intensity on the community size-structure of experimental communities (similar to Fig. 4a). c, f, i, l) Difference between observed and predicted mean abundance for each size-class.

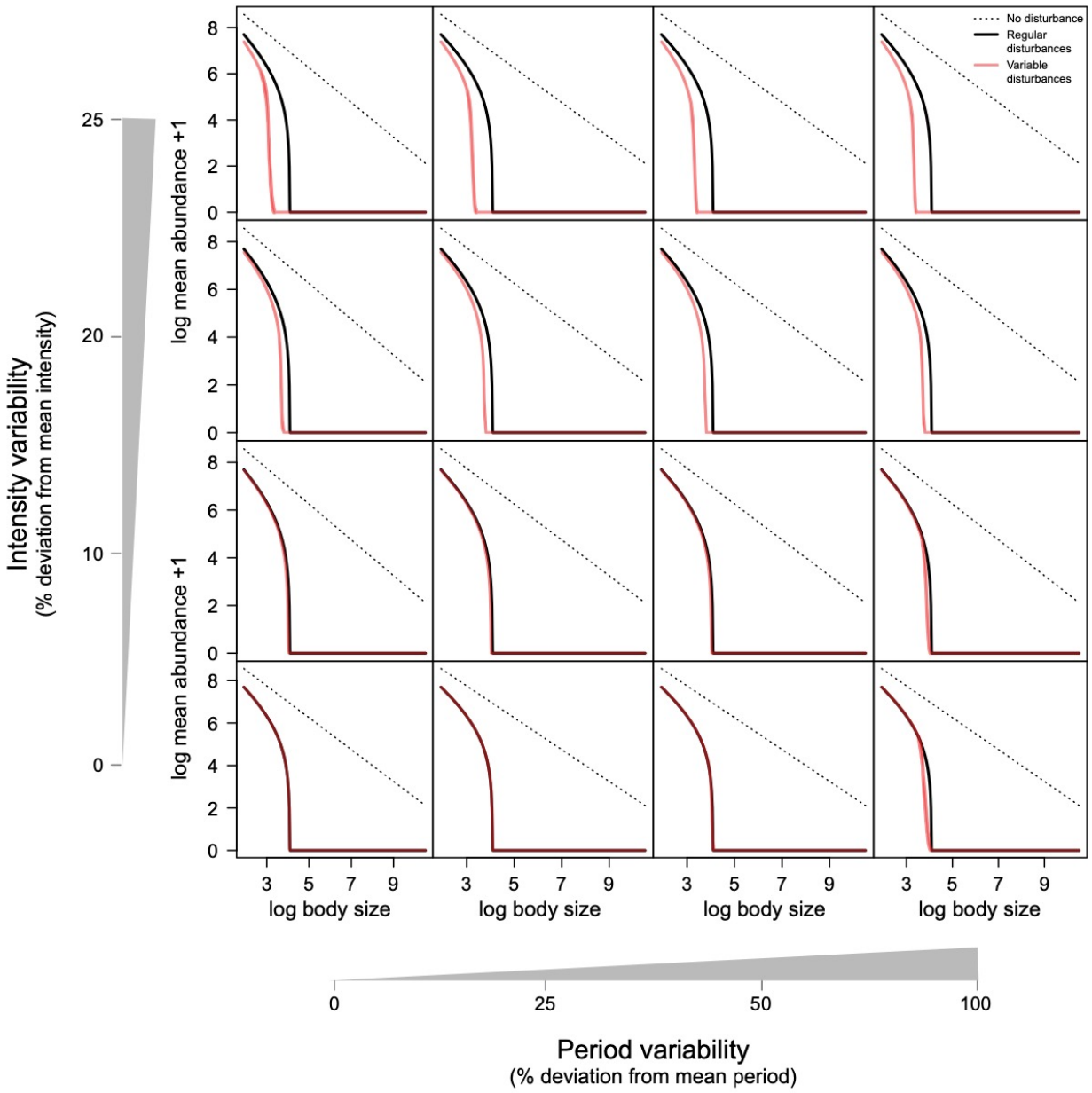

Figure S6: Effect of intensity and period variability on size-abundance pyramids. Community size-structure at dynamical steady state with no disturbance (dotted lines) or disturbances of period 3 (f=0.33) and intensity 80% of abundance reduction, either regular (black lines) or variable (red lines). Red lines give the 95% confidence intervals from one hundred disturbance sequences affecting the same 1000 co-occurring species community during about 10,000-time units. For each disturbance, period and intensity are randomly drawn from uniform distributions in intervals 3±X% and 0.8±Y%, respectively, with $X \in \{0, 25{,}50{,}100\}$ and $Y \in \{0{,}10{,}20, 25\}$. Effects decrease for lower intensities and longer periods (not shown).

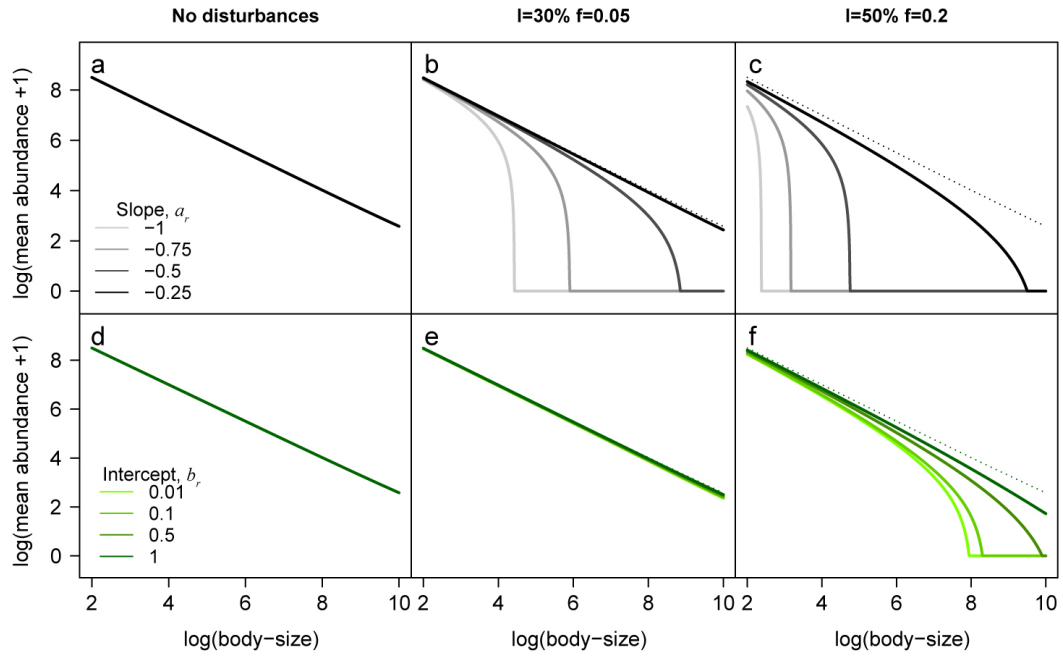

Figure S7: Size-structure response to varying slopes and intercepts of the allometric relationship between population growth rate, r, and body-size, M (equation (12)). **a–c)** Variation of the slope of the relationship, a_r (different greys), with the intercept sets to $b_r = 0.4$. **d–f)** Variation of the intercept of the relationship, b_r (different greens), with the slope sets to $a_r = -0.25$. **a,d)** No disturbances. **b–e)** Small disturbance regime with intensity $I = 30\%$ and frequency $f = 0.05$ (in the same time units than growth rates). **c–f)** Stronger disturbance regime with intensity $I = 50\%$ and frequency $f = 0.2$. Dotted lines in middle and right panels show the size-structure without disturbance (left panels) for comparison. Results are obtained from equation (5).

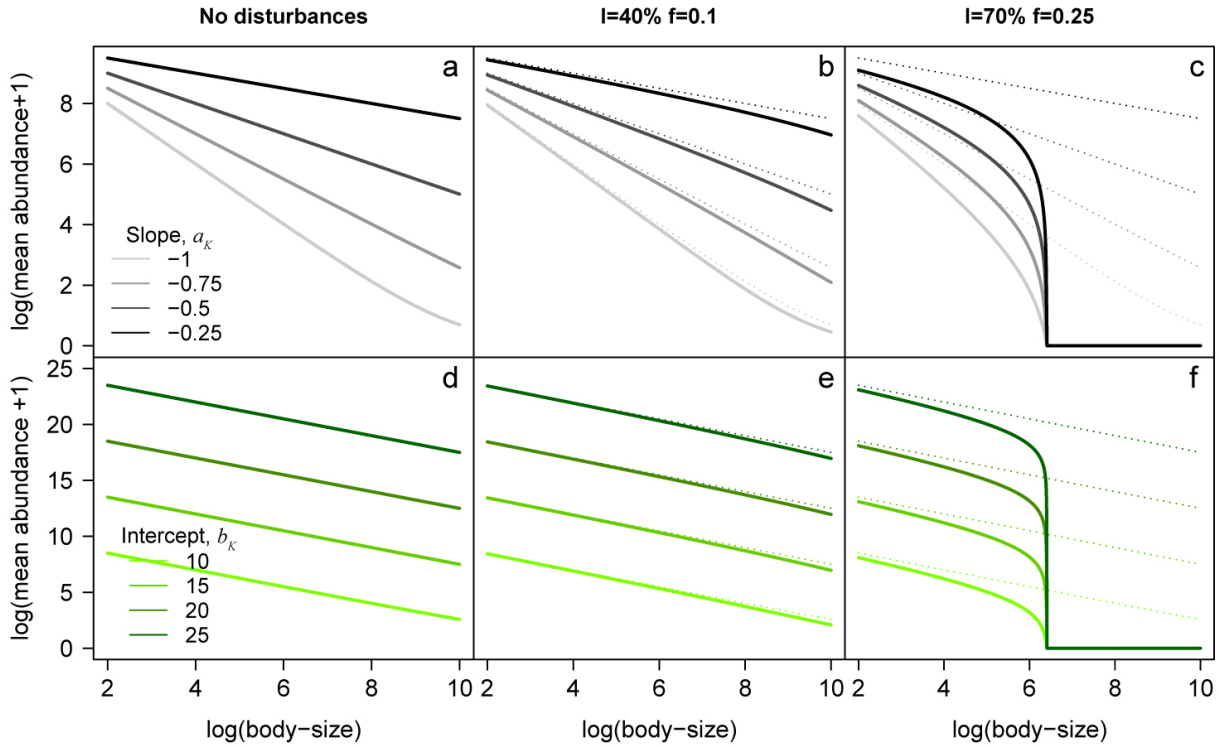

Figure S8: Size-structure response to varying slope and intercept of the allometric relationship between population carrying capacity, *K*, and body-size, *M* (equation (13)). **a–c)** Variation of the slope of the relationship, a_K (different greys), with the intercept sets to $b_K = 10$. **d–f)** Variation of the intercept of the relationship, b_K (different greens), with the slopes sets to $b_K = -0.75$. **a,d)** No disturbances. **b,e)** Moderate disturbance regime with intensity I = 40% and frequency f = 0.1 (in the same time units than growth rates). **c,f)** Stronger disturbance regime with intensity I = 70% and frequency f = 0.25. Dotted lines in panels **b**, **c**, **e**, and **f** show the size-structure without disturbance (left panels) for comparison. Results are obtained from equation (5).

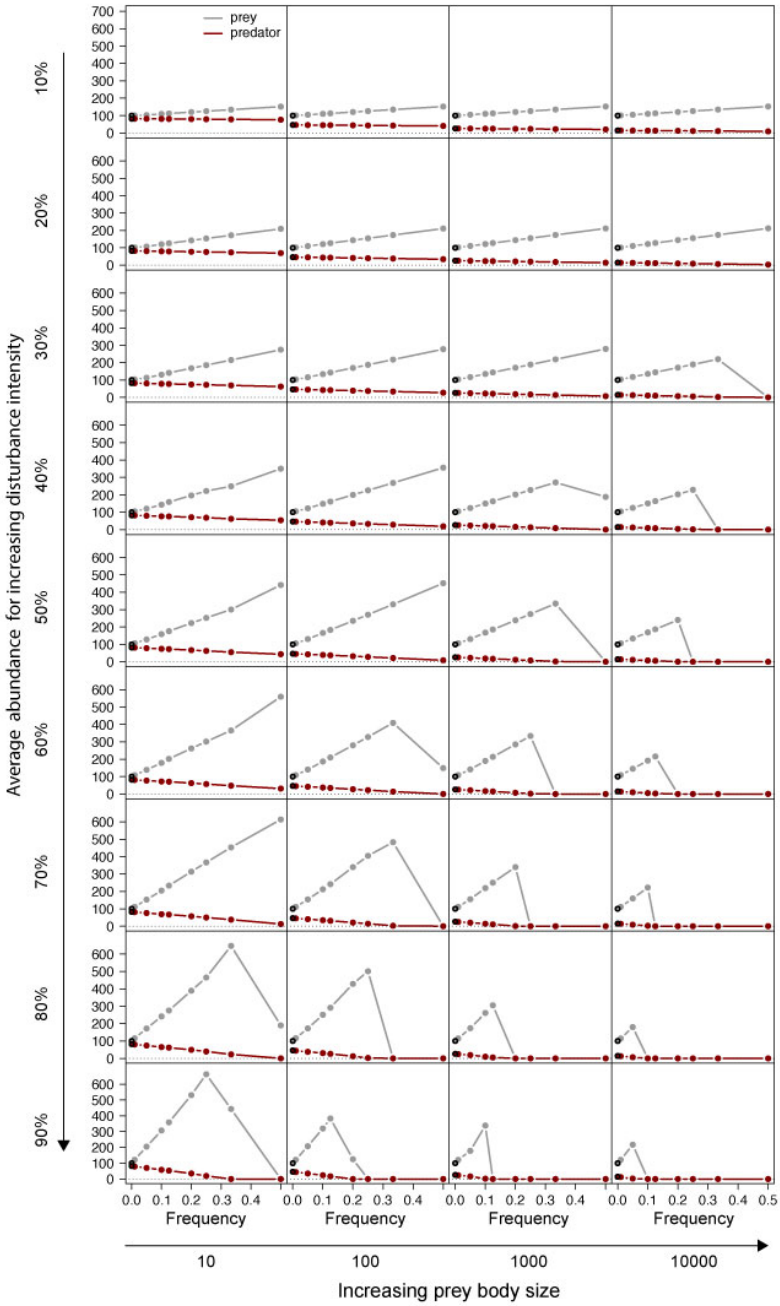

Figure S9: Equilibria for varying disturbance frequency, intensity, and prey size.
Mean abundances at dynamical equilibrium of a Lotka-Volterra predator-prey model submitted to recurrent disturbances of increasing frequencies (x-axis) and intensities (% of punctual abundance reduction in rows), and for different prey sizes (columns). Prey growth rate, r, depends on the body-size, M: $r = e^{-0.25 \times ln(M)+0.5}$. Other parameters are set to: $K = 5000$, $\varepsilon = 0.1$, $a = 0.01$, and $m = 0.1$ (see Table S6). Black circles denote cases without disturbances.

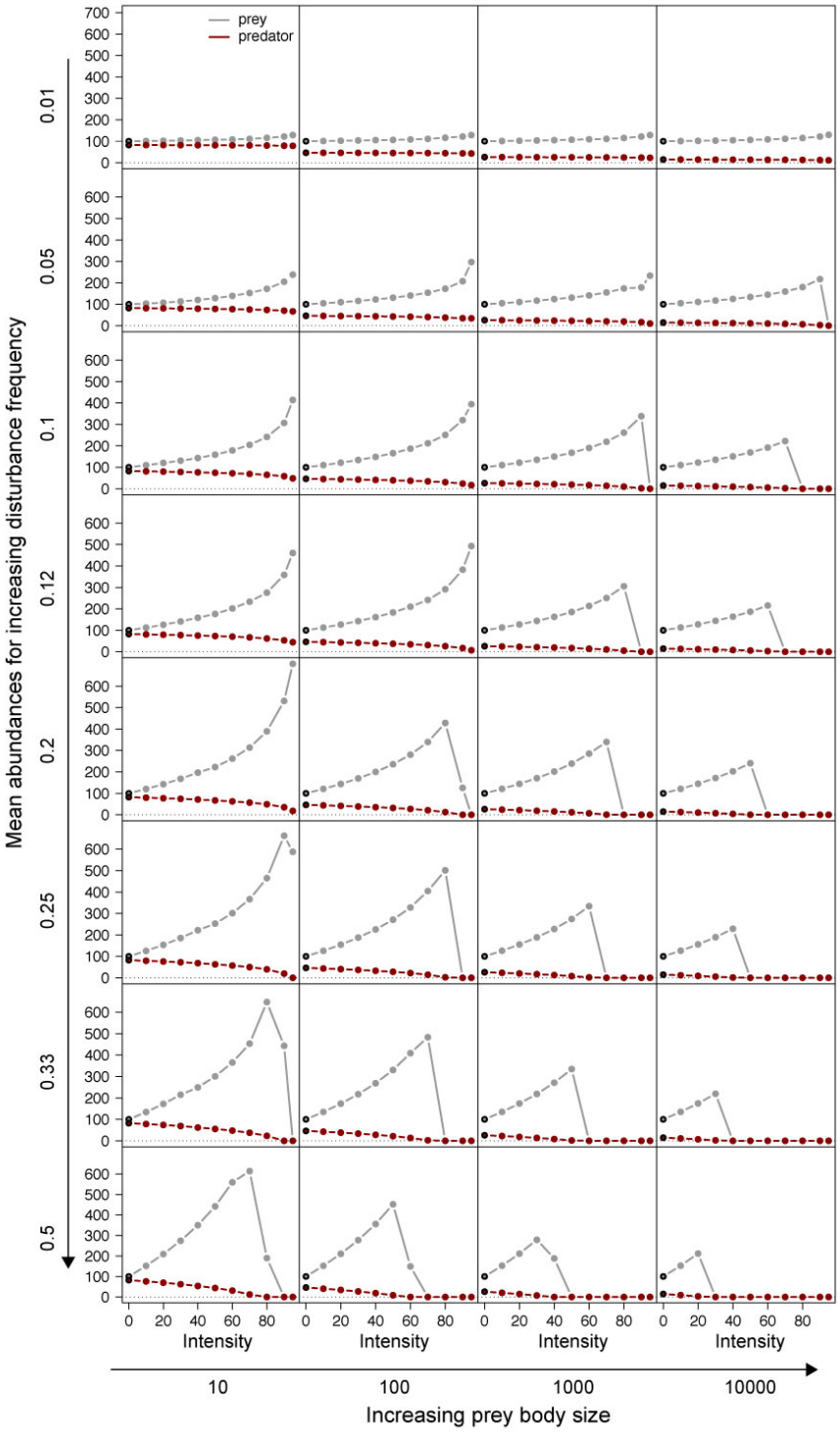

Figure S10: Equilibria for varying disturbance intensity, frequency and prey sizes.
Mean abundances at dynamical equilibrium of a Lotka-Volterra predator-prey model submitted to recurrent disturbances of increasing intensities (x-axis; % of punctual abundance reduction), and frequencies (rows), and for different prey sizes (columns). Prey growth rate, r, depends on the body-size, M: $r = e^{-0.25 \times ln(M)+0.5}$. Other parameters are set to: $K = 5000$, $\varepsilon = 0.1$, $a = 0.01$, and $m = 0.1$ (see Table S6). Black circles denote cases without disturbances.

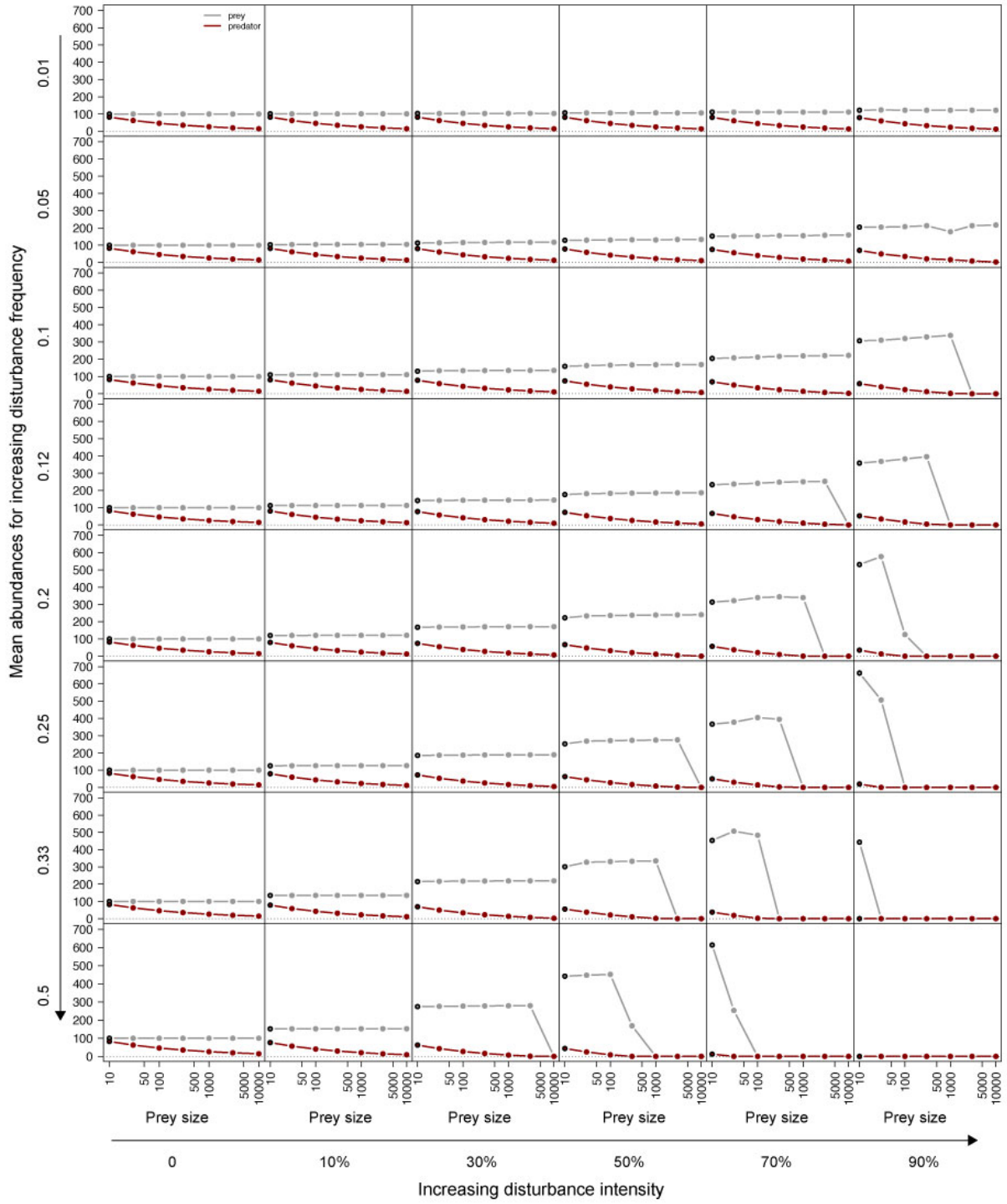

Figure S11: Equilibria for varying prey sizes and disturbance regimes.
Mean abundances at dynamical equilibrium of a Lotka-Volterra predator-prey model submitted to recurrent disturbances, with increasing prey sizes (x-axis) and for different disturbance intensities (columns; % of punctual abundance reduction) and frequencies (rows). Prey growth rate, r, depends on the body-size, M: $r = e^{-0.25 \times ln(M)+0.5}$. Other parameters are set to: $K = 5000$, $\varepsilon = 0.1$, $a = 0.01$, and $m = 0.1$ (see Table S6). Black circles denote cases without disturbances.

7. Supplementary References

Altermatt, F., Fronhofer, E.A., Garnier, A., Giometto, A., Hammes, F., Klecka, J., et al. (2015). Big answers from small worlds: a user's guide for protist microcosms as a model system in ecology and evolution. Methods Ecol. Evol., 6, 218–231.

Brown, J.H. & Gillooly, J.F. (2003). Ecological food webs : High-quality data facilitate theoretical unification. Proc. Natl. Acad. Sci., 100, 1467–1468.

Brown, J.H., Gillooly, J.F., Allen, A.P. & Savage, V.M. (2004). Toward a metabolic theory of ecology. Ecology, 85, 1771–1789.

Carrara, F., Altermatt, F., Rodriguez-Iturbe, I. & Rinaldo, A. (2012). Dendritic connectivity controls biodiversity patterns in experimental metacommunities. Proc. Natl. Acad. Sci., 109, 5761–5766.

Eddelbuettel, D. and Francois, R. (2011). Rcpp: Seamless R and C++ Integration. Journal of Statistical Software, 40(8), 1-18.

Eddelbuettel, D. (2013) Seamless R and C++ Integration with Rcpp. Springer, New York. ISBN 978-1-4614-6867-7.

Eddelbuettel, D. and Balamuta, J. J. (2017). Extending R with C++: A Brief Introduction to Rcpp. PeerJ Preprints5:e3188v1.

Eddelbuettel, D. and Francois, R. (2018). RcppGSL: 'Rcpp' Integration for 'GNU GSL' Vectors and Matrices. R package version 0.3.6.

Galassi, M., Davies, J., Thelier, J. et al, (2001) *GNU Scientific Library Reference* Manual (3rd Ed.), Bristol, 580p, ISBN 0954612078.

Giometto, A., Altermatt, F., Carrara, F., Maritan, A. & Rinaldo, A. (2013). Scaling body size fluctuations. Proc. Natl. Acad. Sci., 110, 4646–4650.

Haddad, N.M., Holyoak, M., Mata, T.M., Davies, K.F., Melbourne, B.A. & Preston, K. (2008). Species' traits predict the effects of disturbance and productivity on diversity. Ecol. Lett., 11, 348–356.

Harvey, E., Gounand, I., Ganesanandamoorthy, P. & Altermatt, F. (2016). Spatially cascading effect of perturbations in experimental meta-ecosystems. Proc. R. Soc. B Biol. Sci., 283, 20161496.

Ryan M. Hope (2013). Rmisc: Ryan Miscellaneous. R package version 1.5.

Pennekamp, F., Schtickzelle, N. & Petchey, O.L. (2015). BEMOVI, software for extracting behavior and morphology from videos, illustrated with analyses of microbes. Ecol. Evol., 5, 2584–2595.

R Core Team (2019). R: A language and environment for statistical computing. R Foundation for Statistical Computing, Vienna, Austria. URL https://www.R-project.org/.

Savage, V.M., Gillooly, J.F. & Woodruff, W. (2004). The predominance of quarter-power scaling in biology. Funct. Ecol., 18, 257–282.